SEPSIS



# A rapid time-resolved host gene expression signature predicts responses to antibiotic treatment in neonatal bacterial sepsis

**Edward C. Parkinson[1]*, W. John Watkins[2], Sarah Edkins[2], James E. McLaren[2], Michelle N. Clements[3], Robert Andrews[2], Federico Liberatore[1], Irja Lutsar[4], Mark A. Turner[5], Emmanuel Roilides[6], Paul T. Heath[7], Michael Sharland[7], Louise F. Hill[7], Peter Ghazal[2], on behalf of the NeoVanc Consortium†**

**Sepsis is a leading cause of mortality and morbidity in neonates yet remains difficult to diagnose. This leads to widespread empiric antibiotic therapy, which can facilitate the development of antimicrobial resistance. How the dysregulated host response to infection and sepsis evolves after antibiotic treatment is poorly understood. Temporal gene expression in neonates with microbiologically confirmed sepsis, treated with the antibiotic vancomycin as part of a randomized controlled trial, was profiled to reveal a treatment-responsive gene signature. The signature exhibited a rapid reversal of the septic state, observable within 24 hours of the initiation of therapy. Unexpectedly, response rates associated with the adaptive immune system were among the fastest, and these changes were reproduced in both pediatric and adult patients with sepsis, indicating conservation and reversibility of sepsis signatures across the life course. We demonstrated how these treatment-responsive genes could be translated into a prognostic clinical measure, exhibiting strong agreement with clinical assessments. Network modeling of sepsis-responsive genes identified a signature associated with treatment comprising an early transient elevation of antimicrobial defensive genes, suggesting an impaired bactericidal response in neonatal sepsis. These findings suggest that the host response is regulated in sepsis and offer insights into early prognostic approaches for reducing antibiotic overuse.**

## INTRODUCTION

Sepsis is the leading pathway to death from infection. Neonates and infants account for the highest burden of sepsis (*1*), with estimates of 5 million cases worldwide each year, resulting in 800,000 deaths (*2*). Late-onset neonatal sepsis occurs in neonates >72 hours of age and, in high-income settings, is most often caused by the hospital-acquired skin commensals coagulase-negative staphylococci (CoNS), with *Staphylococcus epidermidis* the predominant species isolated (*3*, *4*). Although overall mortality rates are low in high-income settings, preterm and low-birth-weight infants often require invasive procedures and supportive care, and neonatal sepsis episodes are associated with morbidity including neurodevelopmental impairments (*5*). The clinical signs of neonatal sepsis can be subtle and highly variable, overlapping with other pathologies. Commonly used tests using inflammatory markers such as C-reactive protein (CRP) and procalcitonin (PCT) exhibit poor sensitivity and specificity for neonatal sepsis (*6*, *7*), and the gold standard diagnostic, a positive microbiological culture from a normally sterile site, can take more than 24 hours and gives a high proportion of false-negative results (*8*). Hence, there is often a low threshold for starting empiric antibiotics (*9*–*11*), resulting in high proportions of neonates exposed to antibiotics, which can potentially cause side effects and affect antimicrobial resistance (*10*, *12*, *13*).

To address these challenges in sepsis diagnosis, host-response transcriptomic biomarkers have been studied extensively. Over the past decade, gene signatures that differentiate patients with sepsis from those with milder disease have been used to both describe the underlying pathophysiology of sepsis at the molecular level and to develop diagnostic and prognostic tools for potential clinical use (*13*–*17*). Multiple neonatal-specific signatures have been reported (table S1). The Sep3 gene signature was derived by comparing the gene expression profiles of 62 neonates (Sep3 discovery cohort), comprising 27 predominantly preterm infants with microbiologically confirmed sepsis (mean gestational age of 31.1 weeks) and 35 predominantly term neonates without suspected infection (mean gestational age of 39.4 weeks), referred to here as uninfected controls (*13*). The Sep3 signature comprises a 52-gene panel attributable to three functional pathway classes—innate immune, adaptive immune, and sugar and lipid metabolism (referred to as metabolic from here on)—where both the innate immune and metabolic pathways are activated in patients with sepsis and the adaptive immune pathway is suppressed. The Sepsis MetaScore (*10*), computed from the expression values of 11 genes and developed using adult and pediatric transcriptomes, is also discriminative in neonates, providing some evidence that neonatal sepsis gene signatures are diagnostic across age groups. More recently, two further signatures have been proposed on the basis of reanalysis of the Sep3 discovery cohort (*18*, *19*). However, the persistence of these biomarkers during the course of sepsis and the potential for these and other biomarkers to monitor response to treatment remain undefined.

[1]Department of Computer Science and Informatics, Cardiff University, Cardiff CF24 4AG, UK. [2]Project Sepsis, Systems Immunity Research Institute, Cardiff University, Cardiff CF14 4XN, UK. [3]MRC Clinical Trials Unit at UCL, London WC1V 6LJ, UK. [4]University of Tartu, 50411 Tartu, Estonia. [5]Institute of Life Course and Medical Sciences, University of Liverpool, Liverpool L7 8TX, UK. [6]3rd Department of Pediatrics, Aristotle University, GR-54124 Thessaloniki, Greece. [7]Centre for Neonatal and Paediatric Infection, Institute for Infection and Immunity, City St George's, University of London, London SW17 0RE, UK.
*Corresponding author. Email: parkinsone@cardiff.ac.uk
†Members of the NeoVanc Consortium and their affiliations are listed after the Acknowledgments.

Host-transcriptomic biomarkers for monitoring clinical recovery from infection have translational applications, including prediction of patient outcomes, early evaluation of treatment efficacy, and personalization of therapy, and have been proposed in a range of infectious disease areas, most notably tuberculosis (*20*, *21*). In sepsis, PCT has been shown to have efficacy as a predictor of treatment response. PCT-guided antibiotic treatment has resulted in reduced antibiotic exposure and lower mortality in adults (*22*) and has facilitated shortening of antibiotic therapy duration in neonates (*23*). However, PCT measurement in neonates can be variable, and standardized ranges for different age groups are lacking (*24*). CRP has also been shown to have utility in measuring treatment responses in adult patients with sepsis in intensive care units (ICUs), with mortality rates differing according to CRP trajectory (*25*). However, CRP is a less reliable marker that has low diagnostic sensitivity in neonates, with concentrations varying dependent on factors such as prematurity or causative organism (*6*, *26*, *27*). A decrease in the host-transcriptome–based quantitative sepsis response signature (SRSq) has been shown to be associated with decreased mortality in adult patients with sepsis. However, no change was observed in cases of pediatric sepsis and septic shock, and the kinetics of individual genes and gene networks were not investigated (*17*). Whether a similar trend can be observed in neonates requires investigation.

The potential for complications from prolonged and unnecessary antibiotic treatment arising from high rates of negative blood cultures and the lack of reliable biomarkers to support a diagnosis, combined with the risk of antibiotic resistance emergence, make host-response biomarkers capable of providing an early indication of treatment response in neonatal sepsis highly desirable. Equally, a deeper understanding of how the septic state is reversed during treatment at the individual gene and gene pathway level may uncover previously unrecognized opportunities for therapeutic intervention. Accordingly, we sought to assess the potential of the Sep3 and other neonatal sepsis gene signatures as treatment monitoring biomarkers in neonatal sepsis and examined the kinetic responses of gene expression in a cohort of neonatal patients from the NeoVanc randomized controlled trial (*28*).

## RESULTS

### Neonatal sepsis signatures are capable of discriminating sepsis events before and after antibiotic treatment

Neonates with a microbiological or clinical diagnosis of late-onset sepsis were recruited into NeoVanc, a randomized noninferiority trial comparing a shorter neonatal-optimized vancomycin regimen, which included a loading dose, with a longer standard course of vancomycin, a widely used antibiotic for Gram-positive late-onset sepsis (*28*, *29*). To ensure as much certainty as possible around the patient diagnosis, this substudy was restricted to patients with a positive culture (of which 96% were CoNS species) and a clinical diagnosis of sepsis. To mitigate the effect of between-patient heterogeneity as a result of the pathogen, a subcohort of infants ($N = 35$) all with confirmed *S. epidermidis* bloodstream infection was selected for analysis. *S. epidermidis* was the most frequently detected CoNS species, present in 69% of NeoVanc patients with a positive culture (*28*). The 35 neonates selected were recruited from 11 of the recruiting tertiary neonatal ICUs across five European countries (Estonia, Greece, Italy, Spain, and the UK). The trial inclusion criteria are provided in tables S2 and S3. Whole-blood samples were taken at the time of recruitment into the trial ($T_R$) and ~3, 5, 10 (standard arm only), and 30 days postrecruitment (table S4), and whole-transcriptome microarray gene expression profiles were produced for all available samples (Fig. 1A). After quality assessment before and after microarray analysis to remove poor-quality RNA and outlier arrays, data for 117 samples were taken forward for analysis. The number of samples available for each of the five time points was 26, 29, 24, 20, and 18, respectively. The resulting transcriptomes provide a temporal profile of the neonatal immune response to infection and subsequent antibiotic treatment.

We first sought to establish whether neonatal sepsis gene signatures have discriminatory power in the NeoVanc patients before and after antibiotic treatment. We reasoned that a major state change in the transcriptome as a result of sepsis should impart similar data characteristics across platforms. Accordingly, a machine learning–based receiver operating characteristic (ROC) classifier (*30*) was trained on the gene expression profiles of the Sep3 genes in the Sep3 discovery cohort and used to classify the NeoVanc participant samples. Samples at $T_R$ were correctly identified as septic with an accuracy of 88% (equivalent to sensitivity given that all patients were septic), and all samples at $T_R + 30$ days (the trial follow-up visit when infants would be expected to have recovered from their septic episode) were identified as nonseptic (Fig. 1B). The classification accuracy was good despite the experimental limitations; the Sep3 discovery cohort was generated with an Illumina microarray platform, whereas the NeoVanc data were generated on the more modern Affymetrix Clarion D microarray platform. Despite centering and scaling the data to correct for these differences, some interplatform variance likely remained (*31*). This, combined with differences in the causative pathogen between cohorts, is likely to affect classification accuracy.

The three patient samples misclassified as nonseptic at $T_R$ may be reflective of a reduced sensitivity and specificity in this population. It is less likely that their positive culture resulted from contamination given the presence of at least three clinical or laboratory signs. No significant difference was observed between the correctly classified and misclassified groups in mean postmenstrual age [$t$ ($t$ statistic) = 0.69; confidence interval (CI) = (−20.8, 41.8); $P = 0.49$] or sex ($P = 0.059$). However, all misclassified patients were among those who received vancomycin in the 24 hours before randomization (fig. S1), which may in part explain their molecular presentation as nonseptic at $T_R$. Within the overall trajectory from septic to nonseptic, individual patient trajectories varied widely (fig. S1). Fast-responding patients achieved a nonseptic classification within the first 72 hours of treatment, whereas it took more than 10 days for slow-responding patients to be classified as nonseptic. No statistically significant difference in the proportions of patients in the optimized compared with the standard vancomycin dosing regimen arm was observed between the fast-responding (classified nonseptic from $T_R + 3$ days onward) and slow-responding (classified septic at $T_R + 10$ days or later) patient groups ($P = 0.60$). Similar analysis was conducted with three other reported neonatal sepsis gene signatures (*10*, *18*, *19*) that achieved a classification accuracy at $T_R$ of 88, 79, and 70%, respectively (figs. S2 to S4). All three failed to identify all patients as nonseptic at $T_R + 30$ days. The Sep3 gene signature achieved the best performance when considering both classification accuracy at $T_R$ and $T_R + 30$ days and thus was taken forward in the analysis. We concluded that previously reported neonatal sepsis gene signatures were effective at discriminating CoNS-induced neonatal sepsis in this subcohort of NeoVanc patients before, during, and after

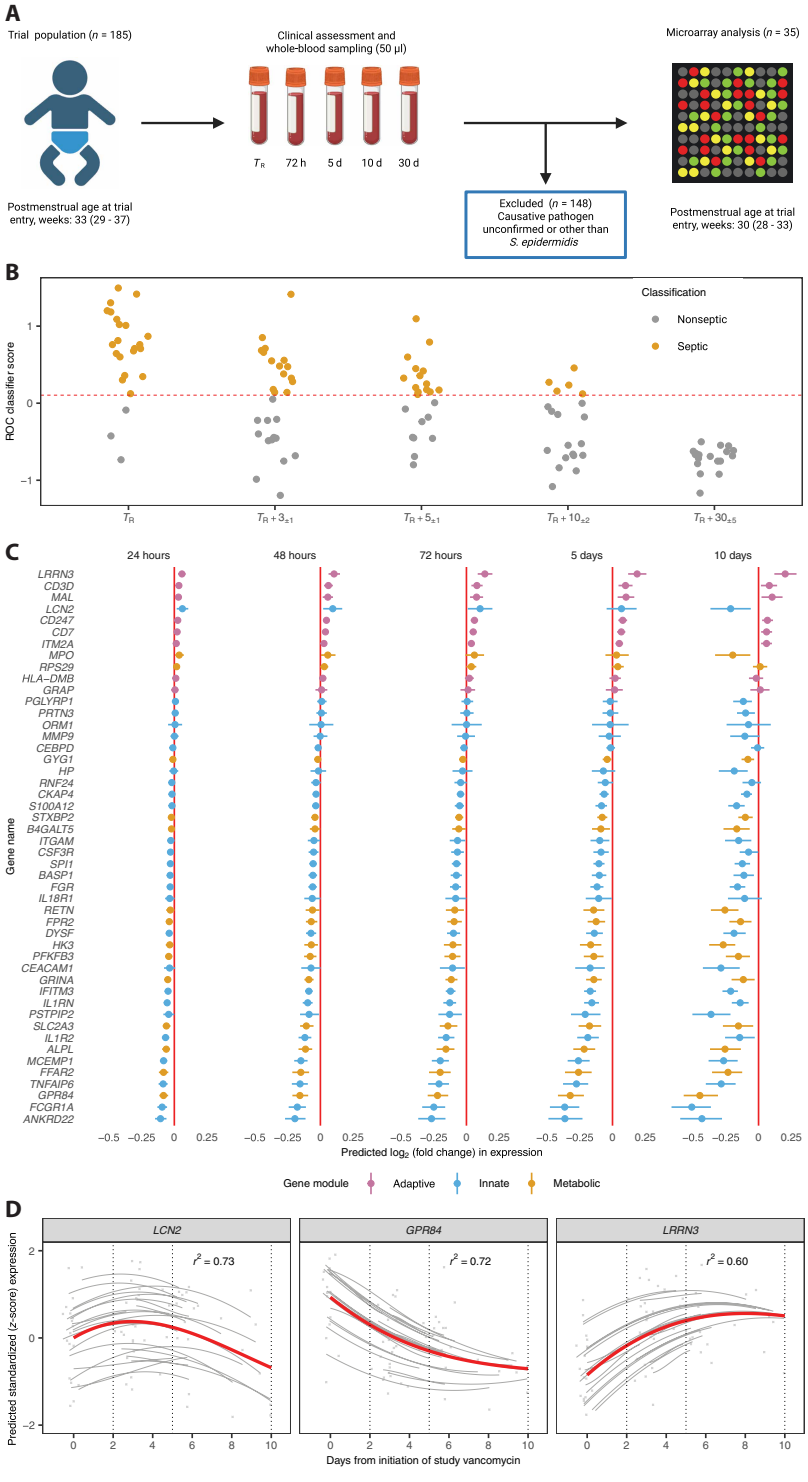


**Fig. 1. Temporal expression profiles reveal immune shift during neonatal sepsis recovery.** (**A**) NeoVanc biomarker study design. Postmenstrual age is given as the median and interquartile range. h, hours; d, days. (**B**) ROC classification of NeoVanc samples using the Sep3 gene signature. Sample collection time points are shown on the *x* axis with the classifier output scores on the *y* axis. Sample points are colored according to the assigned class at each time point ($T_R$: $n = 24$; $T_R + 3$ days: $n = 28$; $T_R + 5$ days: $n = 23$; $T_R + 10$ days: $n = 20$; $T_R + 30$ days: $n = 18$). The red dashed line represents class boundary derived from the Sep3 discovery cohort. (**C**) Mean predicted $\log_2$(fold change) in expression for Sep3 genes at 24, 48, and 72 hours and 5 and 10 days from vancomycin treatment initiation with 95% CIs. Color coding indicates associated immune or metabolic network. $n = 89$. (**D**) Three response subtrajectories illustrated by the modeled expression of *LRRN3*, *LCN2*, and *GPR84* genes in the 10 days after vancomycin treatment initiation. $n = 89$. Mean predictions (fixed effects) in red, and individual patient predictions (fixed plus random effects) in gray, with observed data as gray crosses. Conditional $r^2$ values are shown.

treatment with vancomycin and that the state change from septic to nonseptic was detectable in temporal gene expression profiles.

## Temporal analysis reveals fragmentation of the Sep3 gene signature into responsive and nonresponsive biomarkers

The overall profile of transcriptional change suggested that there were observable, quantitative changes in the expression of individual genes over the treatment course (Fig. 1B). To investigate this, we applied linear mixed regression modeling to the expression profile of each Sep3 gene over the 10-day treatment period to identify features associated with a treatment response. Changes in modeled mean $\log_2$(fold change) expression revealed that 31 of the 48 genes display significant expression shifts during treatment (95% CIs, corresponding to $P < 0.05$; Fig. 1C), with conditional $r^2$ (coefficient of determination) values in the range of 0.355 to 0.772 (mean = 0.619), indicating a good fit for the data. Further details of the modeled expression trajectories, calibration plots of the predicted and observed expression values, and the *P* values and $r^2$ values obtained are provided in figs. S5 and S6 and table S5, respectively. The gene signature split into treatment-responsive and -nonresponsive components, indicating that the underlying pathogenic pathway responses were divergent. The direction of the change in expression of the responsive genes was in the expected direction, based on their functional classes (table S6), and could be divided into three subtrajectories (Fig. 1D). Adaptive immune genes whose expression levels were down-regulated in sepsis [e.g., *CD3D* and *myelin and lymphocyte protein* (*MAL*), both associated with T cell development] recovered toward normal expression values. Innate immune and metabolic pathway genes up-regulated in sepsis [e.g., *G protein–coupled receptor 84* (*GPR84*) and *Fc gamma receptor Ia* (*FCGR1A*; *CD64*), both coding for proinflammatory receptors in myeloid cells] were down-regulated on recovery. The defensive antimicrobial genes *lipocalin 2* (*LCN2*), *myeloperoxidase* (*MPO*), and *peptidoglycan recognition protein 1* (*PGLYRP1*) illustrate a third and unexpected upward then downward trajectory, with expression increasing early in the treatment period and then falling below its $T_R$ value after 10 days. The speed of response to treatment for certain genes in the signature was also unexpected. Modeled mean expression (Fig. 1C) illustrated the rapid change in expression on treatment initiation, with a material proportion of the shift occurring within 48 hours. Unexpectedly, adaptive immune network genes showed some of the fastest responses.

The inclusion of the potential confounding factors sex, birth weight, postmenstrual age, and the administration of antibiotics before randomization as model covariates was examined. The previous administration of antibiotics was significant for two genes, the postmenstrual age was significant for 13 genes at $\alpha < 0.05$, and the goodness of fit, measured by the marginal $r^2$ values, increased in these instances (tables S7 and S8). Innate immune and metabolic genes up-regulated at $T_R$ [e.g., *interleukin 1 receptor antagonist* (*IL1RN*)] naively appeared to have lower expression at $T_R$ in infants who received prestudy antibiotics, suggesting that the curative response may have already begun (fig. S7), and lower expression in older infants (fig. S8). Although these two factors affected the overall expression in a minority of genes, the relationship between gene expression and time from initiation of treatment was unchanged (tables S7 and S8).

To validate that the observed changes in gene expression were not simply the result of changes in immune cell populations, we correlated neutrophil counts with expression of primarily neutrophil-expressed Sep3 genes at each time point. A strong positive correlation was observed at $T_R + 10$ days. However, the correlation was weaker at $T_R$, suggesting that the down-regulation of expression of these genes during treatment response was not simply due to reduced neutrophil numbers but was the result of an immune-mediated down-regulated response (Fig. 2A). We concluded that a component of the Sep3 biomarkers exhibited observable changes early in the treatment period.

## The phenotype shift observed in neonates during treatment is reproducible in independent pediatric and adult cohorts

To establish whether the marked transcriptomic shift observed during treatment of the NeoVanc patients is reproduced in other individuals, we analyzed two independent cohorts of patients with sepsis. Differential expression analysis of a cohort of pediatric patients, comprising 18 controls and 43 patients with sepsis [of which 25 (58%) were microbiologically confirmed, with the most frequent pathogens being *Staphylococcus aureus* and group B streptococcus], at first entry into the pediatric ICU (day 1) (pediatric validation cohort) (*32*), revealed that 49 Sep3 genes were among 4574 differentially expressed genes (fig. S9). The expected down-regulation of adaptive immune and up-regulation of innate immune and metabolic pathways were observed in sepsis samples at day 1 compared with controls (Fig. 2B). A shift in the septic phenotype was observed when comparing day 1 with samples from the same patients with sepsis 48 hours after ICU admission (day 3). Expression of adaptive immune genes was significantly up-regulated [e.g., *Lck interacting transmembrane adaptor 1* (*LIME1*), $P < 0.001$; *leucine rich repeat neuronal 3* (*LRRN3*), $P = 0.032$], whereas innate and metabolic immune gene expression was down-regulated [e.g., *GPR84*, $P < 0.001$; *CEA cell adhesion molecule 1* (*CEACAM1*), $P < 0.001$] (Fig. 2C). A similar rapid shift in expression trajectories was observed in a second cohort of 50 adult patients with septic shock (adult validation cohort), of which 41 (80%) were microbiologically confirmed, and most of those cases were caused by Gram-negative bacteria (*33*). Again, 49 Sep3 signature genes were among the differentially expressed genes identified between patients with septic shock and nonseptic controls (fig. S10). The expected pattern of adaptive immune suppression and innate and metabolic network activation was seen in patients with sepsis at day 1 relative to controls (Fig. 2D). The pattern was reversed 48 to 72 hours after initiation of treatment (Fig. 2E). The specific biomarkers with reversed trajectories at 48 to 72 hours varied between the NeoVanc cohort, the pediatric validation cohort, and the adult validation cohort. However, the network-level pattern was consistent. These rapid changes in a subset of the Sep3 biomarkers, observed in multiple cohorts, led us to conclude that it may be possible to construct a clinically practical measure of treatment response in the early treatment period using these fast-responding biomarkers.

## Shifts in phenotype on recovery can be captured using a treatment response score

To determine whether expression changes in highly treatment-responsive genes could be captured in a dimensionless score, and how well such a measure corresponds to clinical assessments, we defined an immune module ratio (IMR) as the ratio of the median expression of genes down-regulated in response to treatment to the median expression of up-regulated genes. The IMR was calculated for the NeoVanc samples at each time point using a clinically practical subset of 10 genes (five strongly up-regulated and five strongly down-regulated; Fig. 3A). A rapid and significant shift in mean IMR between $T_R$ and $T_R + 3$ days was observed [$t = 4.9$; CI = (0.17, 0.41); $P < 0.001$], which was greater in magnitude than when using all 48 Sep3 genes (fig. S11), suggesting that the full Sep3 diagnostic gene signature is suboptimal for treatment response monitoring and benefits from being optimized for fast-responding markers. To illustrate the magnitude of the transcriptomic shift between the nonseptic state and the septic state at $T_R$, the IMR was calculated using the samples from the short-term follow-up visit at $T_R + 30$ days. This sample was timed to reflect the point by which the neonate should have recovered from their septic episode and ceased receiving antibiotic therapy and thus provided an internal control and proxy for the transcriptomic profile of the infants before the onset of symptoms. Given that 30 of the NeoVanc patients were receiving broad-spectrum antibiotics in the 48 hours leading up to $T_R$, there is a possibility that some of the observed transcriptomic changes around $T_R$ are the host immune response to antibiotic therapy rather than the infection. However, when the pattern of changes in the IMR was analyzed for the five patients who did not receive antibiotic therapy immediately before randomization, similar trends were observed, with a significant difference in the IMR between $T_R$ and $T_R + 10$ days ($P = 0.0062$; fig. S12). This gives some confidence that the transcriptomic profile is the infant's response to the infection. The IMR was also strongly correlated with total sepsis criteria [$\rho$ (Spearman's rank correlation coefficient) = 0.62; CI = (0.47, 0.73); $P < 0.001$], an independent measure of patient recovery, derived from both clinical and biochemical measurements, for each patient at the corresponding time points (Fig. 3B). This correlation was stronger than the correlation between other commonly used measures and total sepsis criteria (excluding the measure tested) such as CRP concentration [$\rho = 0.39$; CI = (0.20, 0.56); $P < 0.001$], blood glucose concentration [$\rho = 0.38$; CI = (0.19, 0.54); $P < 0.001$], and neutrophil count [$\rho = 0.34$; CI = (0.13, 0.51); $P = 0.002$] (table S9). A molecular diagnostic sensitive to host immune recovery in the early treatment period provides information complementary to clinical assessments and blood culture results. A measurable immune shift, indicating reversal of the septic state in patients with persistent positive blood cultures and clinical symptoms (Fig. 3B; patients 27 and 34), may provide confidence in the efficacy of the antibiotic regimen. Equally, evidence of a strong immune response in patients who become culture negative, but whose clinical signs

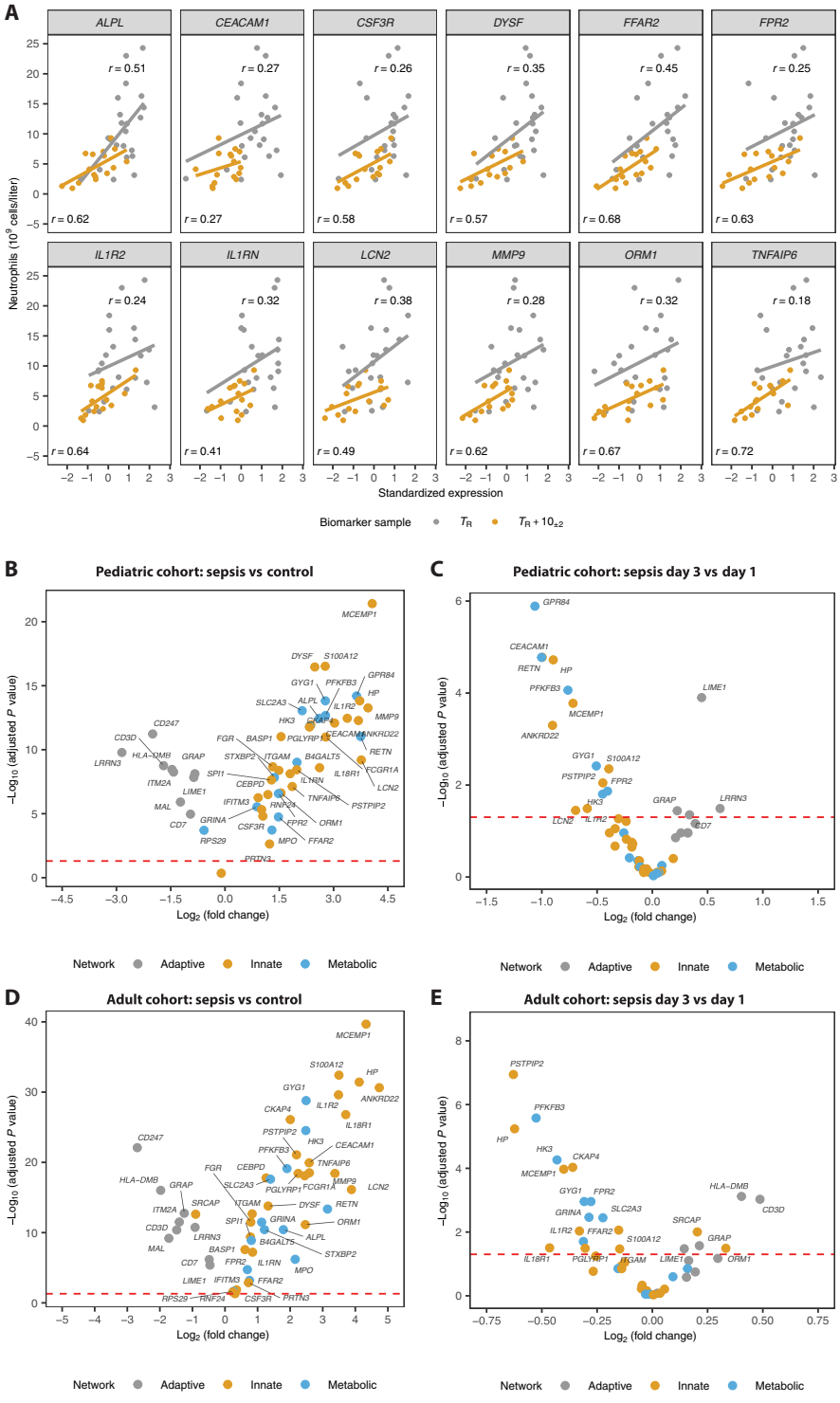


**Fig. 2. The phenotype shift observed in neonates is reproducible in pediatric and adult cohorts.** (**A**) Correlation of expression values of neutrophil-expressed genes (*x* axis) with neutrophil counts (*y* axis) at $T_R$ (gray points) and $T_R + 10$ days (yellow points). The yellow and gray lines are linear least squares regression lines for the respective time points. *r* is the Pearson correlation coefficient. $n = 113$. (**B** to **E**) Differential expression volcano plots comparing pediatric validation cohort day 1 sepsis ($n = 43$) with controls ($n = 18$) (B), pediatric validation cohort day 3 sepsis ($n = 43$) with day 1 sepsis ($n = 43$) (C), adult validation cohort onset of septic shock ($n = 50$) with controls ($n = 22$) (D), and adult validation cohort day 3 of septic shock ($n = 50$) with onset ($n = 50$) (E). Color coding indicates associated immune metabolic network. The red dashed line indicates the *P* value threshold at $\alpha = 0.05$. Significant genes are identified.

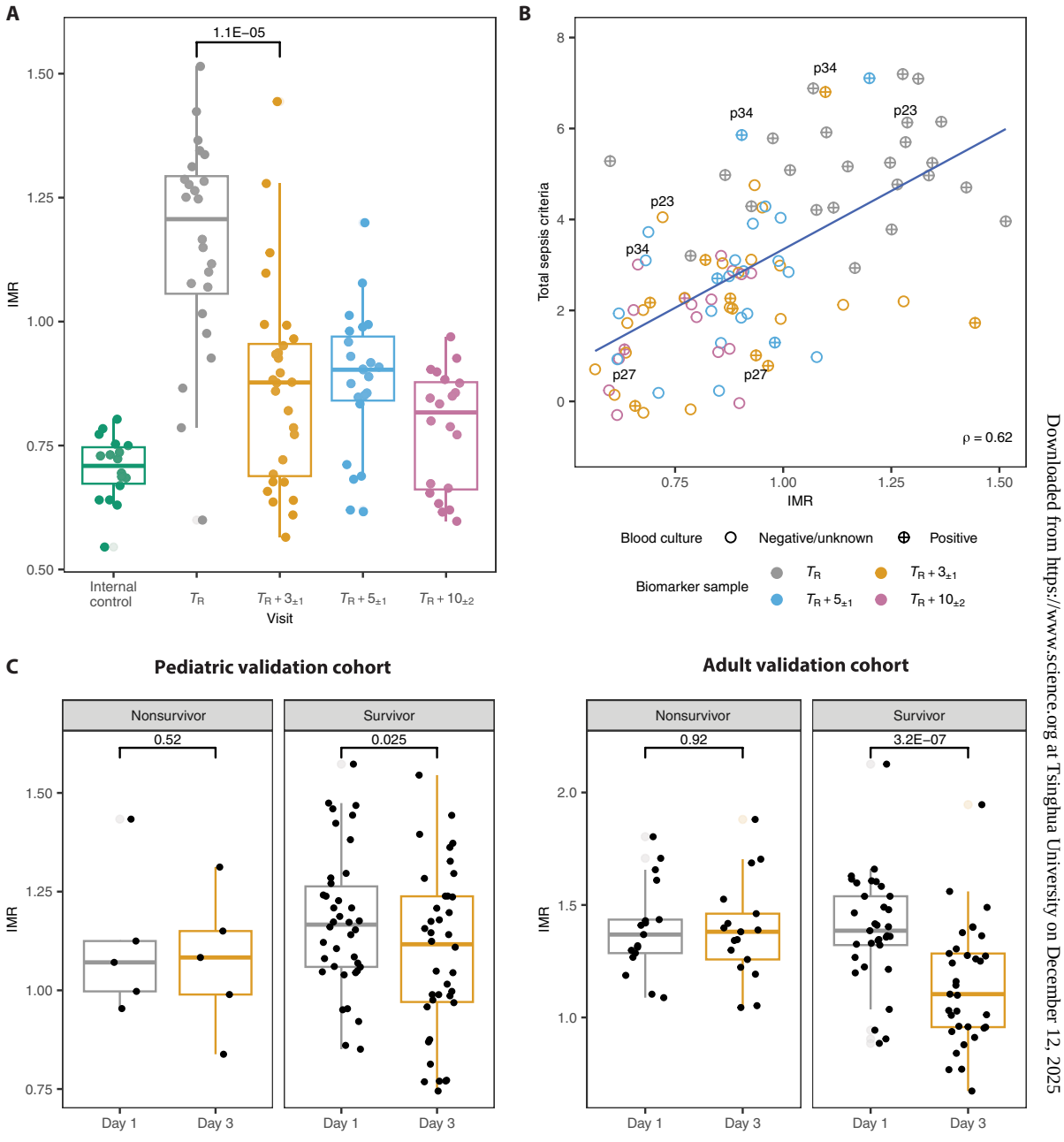


**Fig. 3. Treatment-responsive genes yield a predictive immune response score.** (**A**) Distribution of IMRs calculated with the five most strongly up-regulated and five most strongly down-regulated Sep3 genes for NeoVanc samples. The box-and-whisker plot displays the distribution of IMRs at each time point. The box spans the interquartile range (IQR), from the 25th to the 75th percentile, with the line inside the box denoting the median. The whiskers extend to the smallest and largest values within 1.5 times the IQR from the quartiles. A *t* test–determined *P* value is shown for the difference in mean expression between $T_R$ and $T_R$ + 72 hours. $T_R$ + 30 days are shown as an internal control, representing the assumed range of the IMR before onset of symptoms. $n = 113$. (**B**) Correlation of the IMR with total sepsis criteria. Point color indicates biomarker sample time point. Point shape indicates the existence of a positive blood culture for the patient at or subsequent to the time point. Patients 23, 27, and 34 are labeled for illustration purposes. The blue line is a linear least squares regression line. $n = 113$. (**C**) Distribution of IMRs calculated with the five most strongly up-regulated and five most strongly down-regulated Sep3 genes in the pediatric and adult validation cohorts between day 1 and day 3 sepsis samples. The summary statistics represented by the box-and-whisker plots are as in (A). Paired *t* test–determined *P* values are shown (pediatric: $n = 43$; adult: $n = 50$).

have yet to stabilize (Fig. 3B; patient 23), could result in a reduction in the duration of antibiotic therapy. Furthermore, changes in the IMR in the early treatment period were shown to be indicative of 28-day survival in the pediatric and adult cohorts. Patients were grouped into survivors and nonsurvivors on the basis of outcome 28 days from initial admission. A significant downward shift in the mean IMR, calculated using the same 10 genes as previously, was observed between day 1 and day 3 in the survivor group in both pediatric [$t = 2.34$; CI = (0.01, 0.15); $P = 0.025$] and adult [$t = 6.42$; CI = (0.17, 0.33); $P < 0.001$] cohorts (Fig. 3C). Pediatric and adult patients who did not survive beyond 28 days showed no significant change in the IMR at day 3 [$t = 0.70$; CI = (−0.12, 0.21); $P = 0.52$ and $t = 0.11$; CI = (−0.11, 0.12); $P = 0.92$, respectively]. We concluded that gene expression changes for a fast-responding subset of the Sep3 biomarkers may be used to construct a treatment response measure that is indicative of patient recovery early in the treatment period.

## Modeling all coding genes reveals a shift from an inflammatory antiviral phenotype to a defensive antimicrobial phenotype in response to treatment

The Sep3 signature does not comprehensively explore all functional state changes associated with recovery from sepsis, and it is

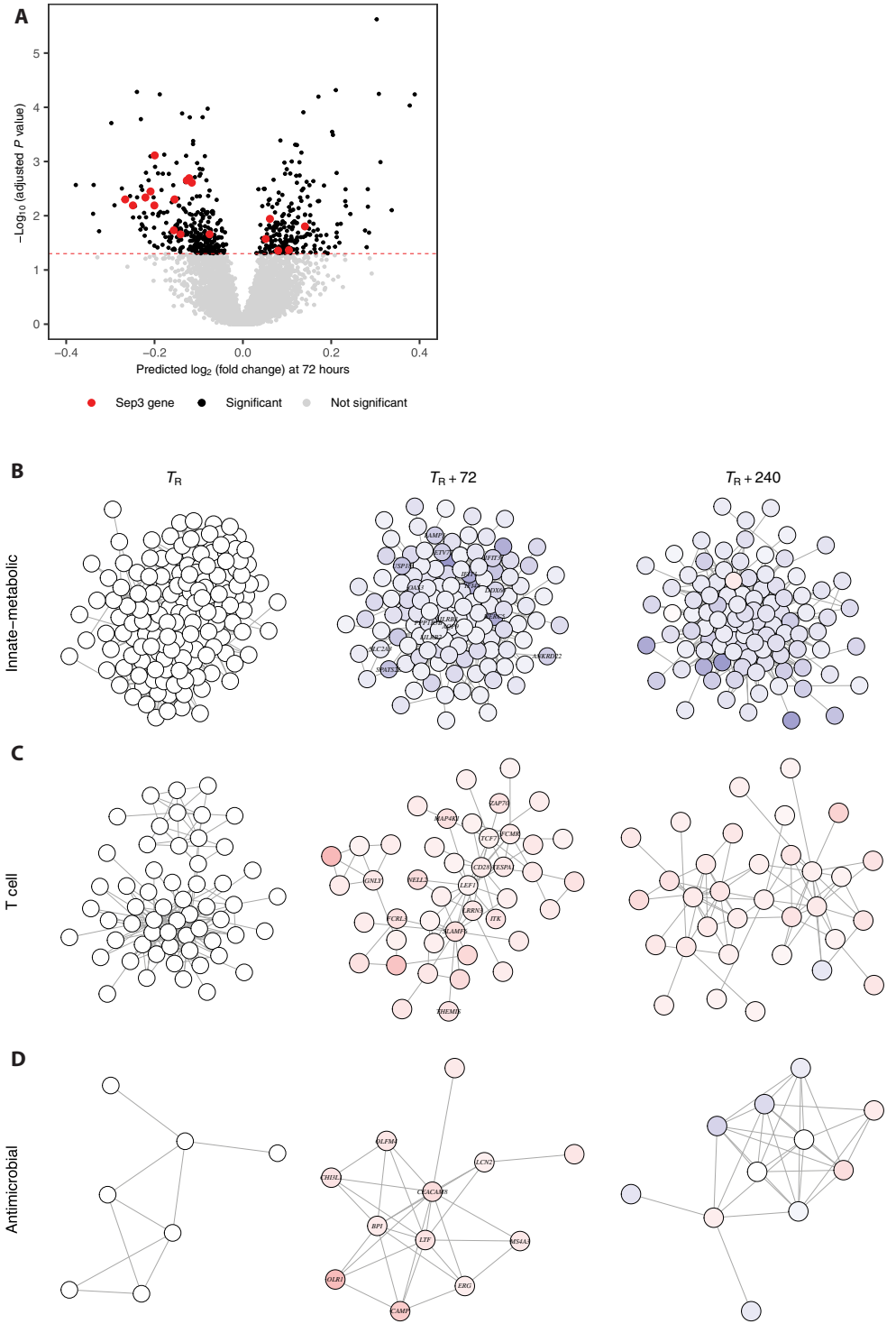


**Fig. 4. Sepsis resolution characterized by a global immune shift with dampened innate and restored cellular responses.** (**A**) Volcano plot showing the predicted $\log_2$(fold change) in expression 72 hours after treatment initiation ($x$ axis) and $-\log_{10}$($P$ value) of the first-order coefficient in the regression model ($y$ axis) for all genes in the NeoVanc dataset. Points representing genes with significant first-order coefficients at $\alpha < 0.05$ are colored black, with the significant Sep3 genes in red. The red dashed line indicates the significance threshold of $\alpha = 0.05$. $n = 89$. (**B** to **D**) Gene correlation networks derived from significant treatment-responsive genes are shown, including an innate-metabolic network (B), a T cell network (C), and an antimicrobial network (D). Nodes represent genes. Gene-gene adjacency measured as topographical overlap. Node color intensity represents $\log_2$(fold change) relative to $T_R$, where red indicates up-regulation and blue indicates down-regulation. $n = 113$.

possible that other pathways and genes may have a more prominent role. Hence, we globally interrogated the treatment recovery response of all coding genes to identify additional biomarkers and signature pathways. Linear mixed regression modeling yielded 422 genes with a significant first-order, second-order, or third-order coefficient with time (for $P < 0.05$) and an effect size similar to or greater than at least one of the Sep3 genes [predicted $\log_2$(fold change) at 72 hours > 0.075] (Fig. 4A).

Network correlation analysis of the expression of this expanded set of treatment-responsive genes at $T_R$, $T_R$ + 72 hours, and $T_R$ + 10 days revealed three distinct and highly interconnected networks: a combined innate immune and metabolic network (Fig. 4B), a T cell network (Fig. 4C), and a third network of predominantly defensive antimicrobial genes (Fig. 4D). During the treatment course, a shift was seen in both the network topology and the predicted gene expression values of nodes in these networks relative to $T_R$ that mirrored the trajectories observed in the Sep3 genes.

The innate-metabolic network remained highly interconnected throughout the treatment course, with expression down-regulated 72 hours after treatment initiation and remaining down-regulated at 10 days. This network could be further subdivided into modules, which were investigated in turn. A module of metabolism-associated genes including *protein phosphatase 1 regulatory subunit 3B* (*PPP1R3B*; glycogen metabolism), *acyl-CoA synthetase long chain family member 1* (*ACSL1*; lipid biosynthesis), *solute carrier family 2 member 3* (*SLC2A3*; glucose transport), and *aquaporin 9* (*AQP9*; lipid transport) was down-regulated, with highly connected hub genes including *ASCL1* and *AQP9* (table S10). The innate response was also down-regulated early on in treatment. Gene expression values for a large module of antiviral defensive genes associated with the type I interferon (IFN) pathway, including those encoding

proteins with stimulatory [e.g., *HECT and RLD domain containing E3 ubiquitin protein ligase 5* (*HERC5*) and *interferon induced protein with tetratricopeptide repeats 1* (*IFIT1*)] and inhibitory [e.g., *ubiquitin specific peptidase 18* (*USP18*)] functions, was down-regulated during recovery. A second innate immune module of leukocyte immunoglobulin-like receptors (LILRs), predominantly myeloid expressed regulators of the innate and adaptive immune response (*34*), also exhibited down-regulated expression early on in treatment. *Leukocyte immunoglobulin like receptor B3* (*LILRB3*; *CD85a*) emerged as one of the most highly connected nodes in the innate-metabolic network, with *LILRB2* (*CD85d*) also highly ranked (table S10), suggesting that these inhibitory immune-related genes may have a regulatory function in the restorative response.

The topology of the T cell network remained tightly connected over the treatment course (Fig. 4C). The unexpected observation that expression of T cell network genes was already up-regulated 72 hours after treatment initiation points to the recovery of T cell proliferation and signaling. These comprised up-regulated expression of cell surface marker *CD28*, possibly indicative of a higher overall T cell population, and expression of genes playing a role in T cell activation and signaling [e.g., *IL2 inducible T cell kinase* (*ITK*), *Fc receptor like 3* (*FCRL3*), and *zeta chain of T cell receptor associated protein kinase 70* (*ZAP70*)]. Up-regulation of expression of genes coding for antigen presenting molecules (*HLA-DQA1* and *HLA-DQA2*) was also indicative of the shift toward a more immunocompetent state. The observed pattern of down-regulation of the innate-metabolic network and restoration of the adaptive immune arm was confirmed by cellular deconvolution analysis (*35*) quantifying the shift in cellular proportions in the NeoVanc samples over the 10 days after treatment initiation: The median $CD4^+$ T cell proportion of total cells increased significantly from 7.3 to 20.1% of total cells [$W$ (Wilcoxon test statistic) = 70, $P < 0.001$], and the B cell proportion increased from 5.7 to 11.2% ($W = 71$, $P < 0.001$), whereas neutrophil proportions declined from 72 to 51% ($W = 407$, $P < 0.001$) (Fig. 5A).

The third, and unanticipated, network of defensive antimicrobial genes was weakly interconnected at $T_R$ with an increase in topological overlap and up-regulated expression at $T_R + 72$ hours. Expression of defensive genes critical to cytotoxic peptide production [e.g., *cathelicidin antimicrobial peptide* (*CAMP*) and *CEACAM8*], pathogen binding [*oxidized low density lipoprotein receptor 1* (*OLR1*) and *CEACAM8*], and bacterial iron sequestration [e.g., *lactotransferrin* (*LTF*) and *LCN2*] were all increased. Gene expression values for these predominantly neutrophil-expressed antimicrobial genes increased during the early treatment period despite overall decreasing neutrophil counts (fig. S13), indicating an immune-mediated up-regulation. At $T_R + 10$ days, the defensive antimicrobial network topology remained highly connected; however, expression was also down-regulated relative to $T_R$, suggesting that the up-regulation of these defensive markers was transitory, relaxing back below $T_R$ values by the end of the treatment period.

The picture emerging from these treatment-responsive genes in the NeoVanc patients can be summarized by changes in five functional modules following three distinct trajectories in response to treatment: T cell signaling (upward recovery); type I IFN, metabolic, and LILRs (downward recovery); and antimicrobial (upward then downward recovery) (Fig. 5B). To investigate whether these signature response modules were replicated in older patients, we conducted differential expression analysis of 47 genes representative of these five modules in the adult validation cohort. Up-regulation of expression of T cell signaling–related genes and down-regulation of expression of metabolic and type I IFN pathway–related genes were observed at day 3 in survivors (Fig. 5C) but not in nonsurvivors (fig. S14). The responses of the LILRs and antimicrobial modules were unclear, with expression up-regulated in some and down-regulated in others in response to treatment. We concluded that there was a regulatory shift during the resolution of the neonatal septic state, with signature pathways indicating a shift from an inflammatory antiviral phenotype to a defensive antimicrobial phenotype. The apparent suppression of antimicrobial defenses observed in the NeoVanc patients, but not clearly replicated in adults, may be related to age or the nature of the causative pathogen.

## DISCUSSION

The data generated in this study provided a time-resolved portrait of the individual gene- and gene pathway–level expression changes taking place during recovery from sepsis. The small-volume PAXgene blood RNA tube collection protocol used required a maximum whole-blood volume of 50 μl (*8*), helping overcome the ethical challenges associated with taking multiple research blood samples from unwell preterm infants. The NeoVanc trial applied this protocol in multiple tertiary neonatal ICUs across Europe, which yielded a sufficient quantity of good-quality RNA to generate the temporal transcriptomic profiles of the 35 neonates.

The previously reported transcriptomic Sep3 biomarkers, which are highly discriminative of sepsis in neonates, have been further validated, including in individuals who were 24 to 48 hours into a septic episode. A potential concern with this result is the difference in gestational age between the septic and uninfected control patients in the Sep3 discovery cohort. This raises the possibility that the ROC classifier used to classify the NeoVanc samples is confounded by gestational age. It is worth noting, however, that, although the Sep3 gene signature was developed by comparing the gene expression profiles of infants of different gestational ages, it was validated by classifying an independent group of 26 infants (16 patients with confirmed sepsis and 10 uninfected controls) with no difference in gestational age, achieving an area under the ROC curve (AUC) of 1.0 (*13*). This validation gives some confidence that the ROC classifier based on the Sep3 gene signature used in this work did not rely on gestational age to discriminate between infants with sepsis and infants who had recovered in the NeoVanc cohort. We have identified a responsive subset of the Sep3 biomarkers that show significant changes in expression over time in response to vancomycin within the first 24 to 48 hours after treatment initiation. These results illustrate the nature of the immune response to antibiotic treatment in neonatal sepsis and the speed with which the septic state is reversed in host recovery. We observed the response from both innate immune and adaptive immune cell markers very early on in the treatment course, with observable changes predicted in the first 24 hours of treatment. The validation of the observed response in the first 48 hours of treatment in both pediatric and adult patients, whose sepsis was a result of infection from a wide variety of species of bacteria, gives some indication that the response is not limited to CoNS sepsis in neonates. The magnitude of the change in this clinically important time window holds promise for these antibiotic

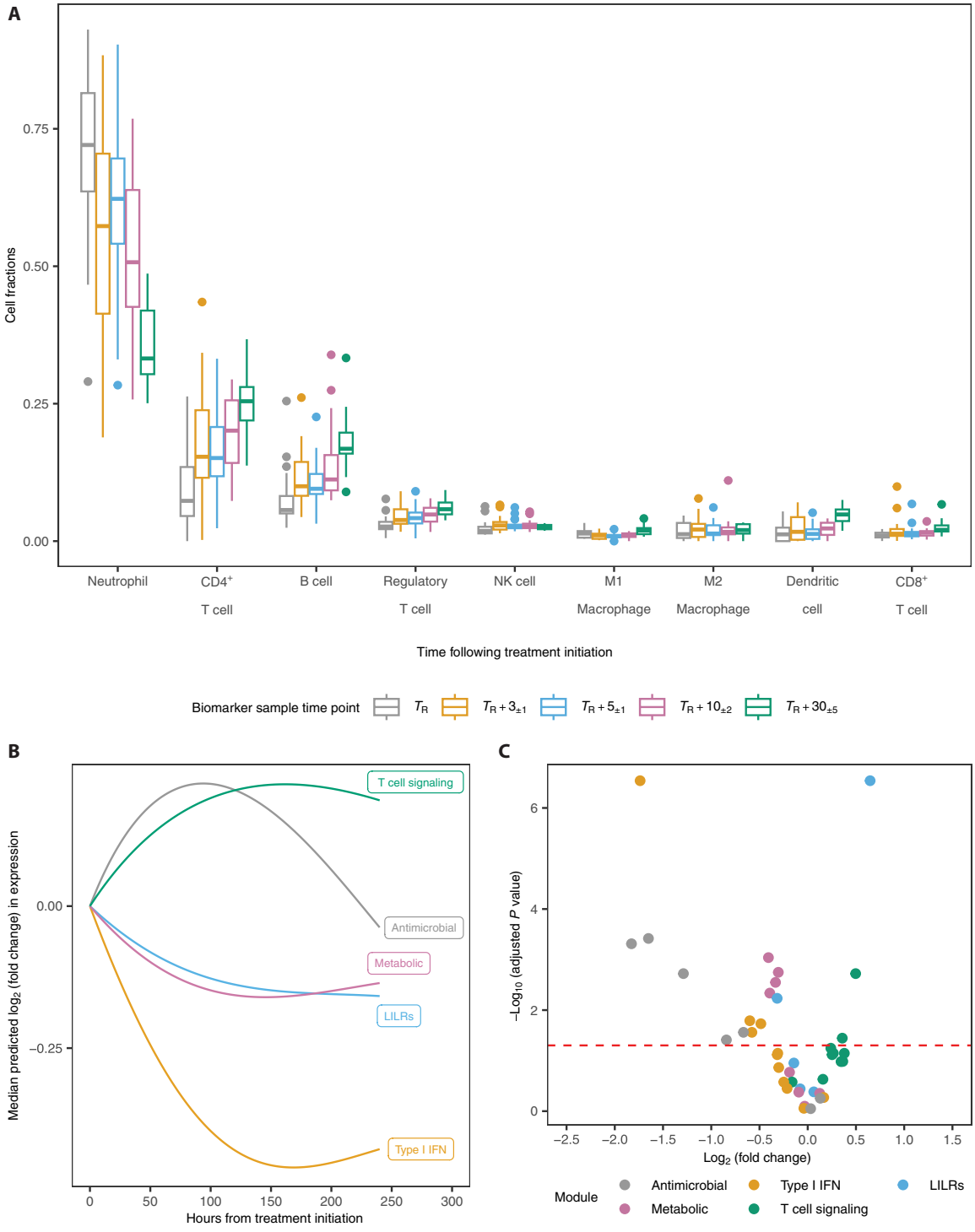


**Fig. 5. Signature pathway expression changes during recovery indicate a shift from an inflammatory antiviral to a defensive antimicrobial phenotype.** (**A**) Estimated cell fractions of key immune cell types over the 10 days after treatment initiation by quanTIseq deconvolution of gene expression profiles. $n = 113$. (**B**) Mean predicted $\log_2$(fold change) expression trajectories of functional gene modules over treatment course. $n = 113$. (**C**) Differential expression of functional module genes between day 3 and day 1 in survivors in the adult validation cohort. $n = 33$. The red dashed line indicates the significance threshold of $\alpha = 0.05$.

responsive biomarkers to be used prognostically as well as diagnostically in the early treatment period. This persistence of the biomarkers in a noncurative state, and then rapid response on treatment with effective antibiotics, suggests that the immune state in sepsis is maintained by continuous signaling from the pathogen and that, as the bacterial load is reduced during treatment, the immune state reverts rapidly. This is suggestive of cooperative behavior between the antibiotic and the immune system; when the antibiotic is introduced, the immune system begins to move to a curative state. This would indicate that the septic state is regulated, rather than dysregulated as commonly defined, and that it can revert quickly.

We have illustrated how the gene expression for a small and therefore clinically practical subset of the Sep3 biomarkers

could be used to create a dimensionless host immune response score. The observed sensitivity of the IMR early in the treatment period, the superior correlation between the IMR and a broad set of clinical and laboratory measures compared with, for example, CRP, and the relationship between early changes in the IMR and 28-day survival together highlighted its translational value. Such a molecular diagnostic would provide clinicians additional information on an infant's recovery and support decision-making around antibiotic therapy at a time when clinical signs may be unclear, with benefits for morbidity, complications, and antibiotic stewardship. The detectable shift in the IMR in pediatric and adult patients with sepsis with heterogeneous causative bacteria, limited to those patients who survived, also provided evidence of the generalizability of the IMR as a treatment response score beyond CoNS sepsis in neonates.

We have described a phenotypic shift observed on recovery in the NeoVanc neonatal subcohort that was characterized by changes in five signature pathways: a marked drop in type I IFN pathway genes early on in treatment, down-regulation of metabolism-related and LILR genes, subsequent recovery of the T and B cellular response, and a rebounding of neutrophil-associated antimicrobial defensive pathways. The observed metabolic shift early in the treatment period is expected, given the high energy cost required to fuel the innate immune response and the resulting high set points for glycolysis and fatty acid metabolism pathways in sepsis (*13*, *36*). The transitory up-regulation of primarily neutrophil-expressed antimicrobial defensive genes provides some evidence that this compartment of the innate immune response is suppressed in the septic state, suggesting that sepsis-induced immunosuppression in neonates extends beyond inhibition of T cell activation and signaling to an impaired inflammatory response, including decreased bactericidal defenses in neutrophils as previously described in adult patients with sepsis (*37*). The observed drop in type I IFN–stimulated genes is suggestive of a reduction in signaling from the pathogen that may be the result of a reducing bacterial load over the treatment course, suggesting that the septic state may be maintained by the presence of the pathogen. Type I IFN production is known to be associated with the suppression of the innate immune response to bacterial infections by increasing the susceptibility of macrophages and lymphocytes to apoptosis-inducing stimuli and by interfering with intracellular bactericidal mechanisms, such as IFN-γ activation of macrophages, aiding bacterial replication (*38*, *39*). It has been reported that expression of IFN-β pathway–related genes is correlative with the extent of disease in leprosy and tuberculosis and that IFN-β may inhibit IFN-γ–induced antimicrobial pathways in these mycobacterial diseases by blocking antimicrobial peptide gene expression of *CAMP* and *defensin beta 4A* (*DEFB4*) (*40*). The concurrent drop in the type I IFN pathway and increase in bactericidal genes observed in our results suggest a similar interaction between these pathways in neonatal sepsis. The precise mechanism may differ from mycobacterial recovery given that we see no up-regulation of IFN-γ pathway genes [e.g., *interferon gamma* (*IFNG*), *interferon gamma receptor 1* (*IFNGR1*), and *C-X-C motif chemokine ligand 9* (*CXCL9*)] in response to treatment.

The emergence of the coinhibitory pathway receptors *LILRB2* and *LILRB3*, previously shown to have up-regulated expression in neonatal sepsis (*13*), as highly connected hub genes in the network topology may also be relevant in understanding the nature of sepsis-induced immunosuppression in neonates. *LILRB2* encodes a potent immunosuppressive receptor known to have a tolerogenic effect in dendritic cells, inhibiting antigen presentation and therefore impairing $CD4^+$ T cell activation and inhibiting the production of reactive oxygen species in neutrophils (*34*). *LILRB2* expression has also been shown to be up-regulated in circulating monocytes and neutrophils in adult patients with septic shock, with increased expression triggered by initial infectious challenge (*33*). The immunosuppressive role of *LILRB3* in sepsis has been demonstrated in mouse models (*41*). LILRB3 was found to inhibit bacterial killing by blocking antigen presentation of macrophages and inhibiting T helper 1 cell differentiation. The same study demonstrated that blocking LILRB3 protected mice from sepsis; the authors speculated that some bacteria can bind LILRB3 expressed on macrophages to inhibit signaling driving downstream bactericidal activity. Murine studies have demonstrated that Gram-positive *S. aureus* is able to bind the LILRB ortholog PIR-B to dampen the host inflammatory response (*42*). LILRB3 has also been reported to be a potent inhibitor of Fc receptor–mediated neutrophil activation, reactive oxygen species production, phagocytosis, and microbial killing (*43*). Our results support the hypothesis that there is a constant signaling between the bacteria and host to maintain the septic state, possibly by exploitation of immunosuppressive LILRs inhibiting $CD4^+$ T cell activation and depressing antimicrobial defenses. The apparent impaired bactericidal defenses in neonates and the potential role of immune checkpoint inhibitors in the recovery process warrant further investigation and raise the question of the potential for therapeutic intervention. A recent murine study demonstrated that high expression of the *IL1RN* immune checkpoint in *Candida albicans*–driven fungal sepsis prevented pathogen clearance and that its targeted removal increased neutrophil recruitment to infection sites and increased resistance to *Candida* (*44*). Our findings point to the potential of similar therapeutic interventions for sepsis that target immune checkpoint inhibitors in bacterial sepsis.

This study has several limitations. The first limitation is the homogeneity of the NeoVanc patients. Given the nature of the NeoVanc clinical trial and the inclusion criteria for this biomarker subanalysis, the results presented primarily investigate the host immune response to staphylococcal sepsis and treatment with vancomycin and not for other pathogens, for example, Gram-negative bacteria, or other specific antibiotics commonly used to treat neonatal sepsis. However, we believe that the results remain highly relevant, given that CoNS species are responsible for 48 to 57% of late-onset sepsis cases in high-income settings (*3*, *4*). In addition, NeoVanc participants could have received other antibiotics, except for the anti-staphylococcal agents flucloxacillin, oxacillin, linezolid, tedizolid, daptomycin, and teicoplanin (*28*), alongside study vancomycin. The results are therefore applicable to the more general neonatal unit population who often receive multiple antibiotics, i.e., with Gram-positive and Gram-negative coverage, at the onset of sepsis. CoNS species are also common contaminants in blood cultures, raising the question of causality between the presence of CoNS and clinical symptoms. We believe it is unlikely that the positive culture results are due to contamination in the NeoVanc cohort. The NeoVanc trial imposed strict inclusion criteria, and all 35 infants had both a positive culture (of which 19 had two or more positive cultures) and three or more clinical or laboratory signs indicative of sepsis. The very high blood culture positivity rates for the study overall (43% culture positive at $T_R$) indicate that the inclusion criteria were successful in selecting neonates with sepsis. In addition, 80% of the neonates included in

the NeoVanc trial were preterm, 65% were very low birth weight, and 40% were extremely low birth weight, making this a population at the highest risk of CoNS sepsis (*45*).

A further limitation is that all patients in the subcohort ultimately recovered. This raises the question of whether the observed immune response was a direct result of vancomycin therapy, as opposed to other clinical interventions, or simply the progression of sepsis. We also believe it is unlikely that most of these infants would have had a favorable clinical outcome without antibiotic treatment. Although the overall mortality for CoNS is low, mortality rises to ~9% in very-low-birth-weight and preterm infants (*45*). Thirty-four of the 35 infants selected for this study were preterm infants, and of those, 25 had very low birth weight, making this a highly vulnerable population. This, combined with the fact that antibiotic susceptibility testing revealed vancomycin-susceptible *S. epidermidis* in all patients, gives some confidence that the recovery of these patients was a result of the vancomycin therapy. Conversely, in the absence of a nonseptic control group receiving prophylactic antibiotics, we acknowledge that we cannot be certain that the observed gene expression trajectories are not in part due to the effect of vancomycin itself. However, the similar transcriptomic pattern observed between those patients who did and those who did not receive antibiotics in the 48 hours before randomization goes some way to indicate that the antibiotics themselves are not the primary driver of the transcriptomic shifts. Further work is required to validate that the treatment response and signature pathways observed in the NeoVanc subcohort are reproduced in larger and more diverse neonatal cohorts. Translation of the IMR into a clinical setting will also require further work to optimize the subset of biomarkers selected and to both validate and calibrate the score in a larger patient population.

We conclude that there is a marked shift in regulatory gene expression during the resolution of the septic state. We observed a change in the overall regulatory set point, transitioning from an inflammatory antiviral phenotype to a defensive antimicrobial phenotype. Moreover, this shift was observed very early in the treatment course in neonates as well as pediatric and adult patients, suggesting that the pattern persists throughout the life course. The observed speed of this systemic change raises the prospect of prognostic tests to provide an early indicator for sepsis treatment response in the clinic.

## MATERIALS AND METHODS

### Study design

The purpose of this study was to investigate changes in host gene expression profiles of neonates with sepsis during vancomycin therapy. The study analyzed data from a subset of the infants recruited to the NeoVanc trial, a multicenter randomized open-label phase 2b study that compared the efficacy, safety, and pharmacokinetics of an optimized dosing with a standard dosing regimen of vancomycin in neonates and infants aged less than 90 days with late-onset bacterial sepsis (ClinicalTrials.gov ID: NCT02790996) (*45*). NeoVanc and this biomarker subanalysis were approved by the London–West London and Gene Therapy Advisory Committee (REC reference [16]/LO/1026) on 18 July 2016. Ethics committee and regulatory body approvals were obtained for each participating hospital. Written informed consent was obtained from all patients' parents or guardians. The study was performed in accordance with the International Conference on Harmonisation of Technical Requirements for Registration of Pharmaceuticals for Human Use Good Clinical Practice guidelines, local regulations, and standard operating procedures. Infants were randomly assigned to the trial arms; infants in the optimized dose arm received vancomycin for 5 ± 1 days, whereas infants in the standard arm received vancomycin for 10 ± 1 days; no infants received more than 24 hours of vancomycin before randomization. Trial inclusion criteria are detailed in tables S2 and S3, and full details of the trial protocol are provided by Hill *et al.* (*45*). Thirty-five infants were retrospectively selected for this substudy. The sample size was determined by the availability of trial patients with microbiologically confirmed late-onset sepsis caused by the pathogen *S. epidermidis*. The group comprised 18 male and 17 female patients selected from 11 of the recruiting tertiary neonatal ICUs across five European countries (Estonia, Greece, Italy, Spain, and the UK). A list of these recruiting sites and the corresponding investigators is provided in table S11. Whole-blood samples were taken for microarray gene expression profiling. Infants whose therapy followed a trial protocol were sampled four times in the optimized arm and five times in the standard arm; those whose vancomycin therapy ended earlier or later than outlined in the protocol were also sampled at the end of vancomycin therapy (EVT) time point (table S4). Given the blood volumes available in this vulnerable population and the cost of transcriptomic analysis, a single experimental replicate was used for each infant at each time point. Detailed clinical (e.g., temperature and heart rate) and laboratory (e.g., white blood count, CRP, blood glucose concentrations, and blood culture results) measurements were also collected at the same time points. Blood samples were processed for microarray gene expression profiling as discussed below. Blood samples with an RNA Integrity Number (RIN) value of >5 were included for microarray analysis. Quality assurance of Affymetrix cell intensity file (CEL) data by statistical testing yielded eight outlier arrays before robust multiarray average (RMA) normalization, and a further seven samples after normalization. A further outlier sample was identified on the basis of suspected mislabeling. All outlier samples were excluded from analysis. The resulting dataset facilitated temporal analysis of gene expression changes in response to vancomycin therapy and cross-validation of the observed changes with clinical observations and laboratory readings.

### NeoVanc trial dataset

The NeoVanc dataset comprises microarray gene expression data for 35 infants, a subset of the infants recruited to the NeoVanc trial. Whole-blood samples were taken, following a small-volume PAXgene blood RNA tube (Thermo Fisher Scientific) collection protocol (*8*) requiring a maximum of 50 μl of whole-blood volume, at time points outlined in table S4. Total RNA quality and quantity were assessed using Agilent 4200 TapeStation and a High Sensitivity RNA kit (Agilent Technologies). Two to 10 ng of total RNA with an RIN value of >5 was arrayed into a 96-well plate format and hybridized to the Thermo Fisher Scientific Clariom D microarray using the pico GeneChip labeling kit. First-strand cDNA was synthesized with a combination of a Poly-dT and random primers containing a 5′-adaptor sequence. A 3′-adaptor was added to the single-stranded cDNA followed by low-cycle polymerase chain reaction (PCR) amplification. The cDNA was used as a template for in vitro transcription (IVT) that produced amplified amounts of antisense messenger RNA (cRNA). The cRNA was then used as input for a second round of first-strand cDNA synthesis, producing single-stranded

sense cDNA. After fragmentation and end-labeling, the targets were hybridized to plate arrays, which were stained and imaged on the GeneTitan MultiChannel Instrument. Raw cell intensity file (CEL) data were read into R version 4.1.2 and analyzed for quality using the arrayQualityMetrics package (*46*). Potential outliers, in particular arrays with very low amounts of hybridization, were identified by visual inspection of box plots of raw expression values and calculating the value of the nonparametric Kolmogorov-Smirnov test statistic, comparing each sample with a reference of all samples. Outliers were identified for further investigation on the basis of values greater than 1.5 times the interquartile range (*47*), and eight samples were excluded from further analysis. Raw intensities were normalized with the RMA method using the oligo package (*48*) and annotated with a National Center for Biotechnology Information (NCBI) gene name using the annotateEset() function from the affcoretools package (*49*) with the Affymetrix clariomdhuman annotation data package clariomdhumantranscriptcluster.db version 8.8.0 (*50*). Only probe sets mapped to an NCBI gene name were retained, and maximum average intensities were taken over replicate gene names. Potential outlier samples following RMA normalization and probe summarization were again investigated using the arrayQualityMetrics package, using comparative metrics widely used in microarray datasets (*51*): (i) the total L1 (Manhattan) distance of each sample's counts from all other samples; (ii) the value of the nonparametric Kolmogorov-Smirnov test statistic, comparing each sample with a reference of all samples; and (iii) Hoeffding's *D* statistic, a nonparametric measure of the independence of the $\log_2$ ratio and the $\log_2$ average of intensities between each sample and a reference of all samples. Outliers were identified on the basis of values greater than 1.5 times the interquartile range in at least two of these three tests, and seven further samples were excluded from further analysis. Low-intensity genes with a $\log_2$ transformed intensity of 3 or below in all samples were removed. The low-intensity threshold was set on the basis of visual inspection of a histogram of the distribution of $\log_2$ transformed intensities based on the procedure outlined in (*52*). A further sample was excluded from analysis on the basis of suspected mislabeling of the blood collection tube.

### Sep3 discovery cohort

The Sep3 discovery cohort microarray dataset (*13*) was obtained from the NCBI Gene Expression Omnibus (GEO) database (GSE25504). The data were generated by hybridizing RNA from 63 infected and control infants onto Illumina Human Whole-Genome Expression BeadChip HT12v3 microarrays comprising 48,802 features (human gene probes). Raw data from 63 samples were transformed using a variance stabilizing transformation before robust spline normalization to remove systematic between-sample variation. Full details are provided in (*13*). A single sample (Inf075) identified as a viral infection was excluded from the analysis. Illumina HT12 platform gene probes were mapped to ensembl transcript IDs and NCBI gene names using the ensembl database (*53*); only those probes mapping to an ensembl transcript ID were retained, and the transcript ID with the maximum average normalized expression for each gene name over all samples was retained as the representative expression for each gene. Expression values were standardized (*z*-scored).

### Pediatric validation cohort

The pediatric validation cohort microarray dataset (*32*) was obtained from the NCBI GEO database (GSE13904). Raw CEL data were read into R version 4.1.2 and analyzed for quality using the arrayQualityMetrics package (*46*) as previously described. The microarray data, generated using the Human Genome U133 Plus 2.0 GeneChip, were summarized using RMA and combined with clinical metadata received directly from the H. Wong research group. Probe sets were annotated with an NCBI gene name using the annotateEset() function from the affcoretools package (*49*) with the annotation data package hgu133plus2.db version 3.13.0 (*54*). Only probe sets mapped to an NCBI gene name were retained, and maximum average intensities were taken over replicate gene names. Independent filtering was conducted to remove low-intensity genes ($\log_2$ intensity of 4 or below in all samples), low variance genes (genes below 50th variance percentile), and all noncoding genes. The data were further processed by removing samples classified as having systemic inflammatory response syndrome (SIRS) and as "SIRS resolved." Samples classified as "Sepsis" and "Septic Shock" were combined as sepsis. Only those patients with confirmed bacterial sepsis or no microbiologically determined cause of infection were retained; patients with confirmed viral and fungal infections were removed. The causative pathogens in microbiologically confirmed patients included both Gram-positive and Gram-negative bacteria. In addition, only those patients with sepsis with samples for both day 1 and day 3 were retained, leaving 43 patients with sepsis with both day 1 and day 3 samples alongside 18 noninfected day 1 control samples.

### Adult validation cohort

The adult validation cohort microarray dataset (*33*) was obtained from the NCBI GEO database (GSE95233). Raw CEL data were read into R version 4.1.2 and analyzed for quality using the arrayQualityMetrics package (*46*) as previously described, and two samples were identified as outliers. The microarray data were generated using the Human Genome U133 Plus 2.0 GeneChip and summarized using RMA. Probe sets were annotated with an NCBI gene name using the annotateEset() function from the affcoretools package (*49*) with the annotation data package hgu133plus2.db version 3.13.0 (*54*). Only probe sets mapped to an NCBI gene name were retained, and maximum average intensities were taken over replicate gene names. Independent filtering was conducted to remove low-intensity genes ($\log_2$ intensity of 4 or below in all samples), low variance genes (genes below 50th variance percentile), and all noncoding genes. The dataset contained gene expression data for 51 patients with septic shock (reduced to 50 after outlier sample removal), sampled at admission (day 1) and either 2 or 3 days later, and 22 healthy controls. All patients were over the age of 18. For the purposes of analysis, days 2 and 3 were combined as a single time point (day 3). Forty-five of the patients with septic shock were confirmed as being infected with Gram-negative or Gram-positive bacteria (*33*). It was not possible to identify the patients without confirmed bacteremia from the data available; therefore, all 50 patients were retained in the analysis. Septic shock was defined as the beginning of vasopressor therapy in combination with an identifiable site of infection, persisting hypotension, and evidence of a systemic inflammation.

### Sample classification

Of the 52 genes originally identified in the immune-metabolic classifier in (*13*), 48 were reliably mapped to probe sets in the NeoVanc dataset. This 48-gene subset is detailed in table S6 and referred to as the Sep3 gene signature throughout this article. The four genes that could not be reliably mapped to probe sets in the Affymetrix

Clariom D array were *SRCAP*, *TRAJ17*, *LIME1*, and *TRBV28*. A ROC-based classifier (*30*) was trained on the 62 samples of the Sep3 discovery cohort using the R package rocc, with the Sep3 genes as input variables. A single patient who died 10 days after randomization into the trial was excluded from the NeoVanc subcohort (patient 14) on the basis that this patient is unlikely to be representative of a patient responding to vancomycin treatment. The trained ROC classifier was then used to predict whether each NeoVanc sample was septic or noninfected.

### Linear mixed regression modeling

Linear mixed regression models (LMRMs) that describe the trajectory of gene expression for each gene individually over time were fit and analyzed using the R package lme4 (*55*) and *P* values derived using the R package lmerTest (*56*). Two criteria were applied to filter the set of 35 patients for inclusion in the LMRM analysis: (i) The patient survived beyond the day 30 short-term follow-up visit (patient 14 excluded), and (ii) data for at least three biomarker samples were available given the desire to fit models including quadratic and cubic terms (11 patients excluded). The resulting 23 patients were included in the LMRM analysis. Independent filtering based on median intensity and variance was conducted before LMRM analysis of all genes in the NeoVanc dataset to reduce the impact of multiple testing. Noncoding genes were also removed before analysis.

We intuitively expected gene expression to follow a monotonic saturating lowering or elevating trajectory over time, reaching a steady state on resolution of the infection; therefore, the optimal mean model was investigated by applying simple linear regression to the expression data for each gene and evaluating adjusted $r^2$ and Akaike information criterion (AIC) values for three alternative base models with the following variables: (i) *time*; (ii) $time + time^2$; (iii) $time + time^2 + time^3$. Models including quadratic and cubic terms yielded consistently better model fits (table S12) and hence were selected as the optimal mean model. An intraclass correlation coefficient (ICC) was calculated for each gene using an unconditional means model (table S13). The mean ICC of 0.284 indicated that, on average, ~30% of the expression variance was explained by between-patient effects, highlighting the patient heterogeneity in gene expression and justifying the modeling of mixed effects to provide more consistent and stable parameter estimates for the effects of time on gene expression.

LMRMs included scaled (*z*-scored) expression as the response variable, obtained using the mean and SD of the expression values over all patients and time points for the gene. The fixed effects covariates comprise the linear and polynomial terms *time*, $time^2$, and $time^3$ to model the mean curved trajectories of gene expression changes. Data for biomarker samples taken at $T_R$, $T_R + 72$ hours, $T_R + 5$ days, and $T_R + 10$ days were included, covering the treatment period. Data for the biomarker sample taken at $T_R + 30$ days were excluded from the LMRM analysis given that this sample was taken beyond the end of treatment period. LMRMs were fit with random intercept and random slope terms to model heterogeneity in starting expression values and rate of change of expression over time between patients. The approach to the random effects design follows principles outlined by Barr *et al.* (*57*). Models were initially fit for all genes with random intercept and random slope as random effects covariates. In the case a model with both random slope and random intercept terms resulted in a singular fit, the design matrix was simplified to a random intercept only model and refit; where a random intercept only model failed to converge, the gene was excluded from the analysis. The intercept and slope terms were assumed to be correlated using the default unstructured variance-covariance structure in the lme4 implementation, and the model was fit using the residual maximum likelihood (REML) method. CIs were calculated for the predicted mean and $\log_2$(fold change) using randomized bootstrapping over 1000 iterations with the bootMer function in the lme4 package. Adjusted *P* values for linear and polynomial coefficients were corrected for multiple testing by applying the Benjamini-Hochberg procedure (*58*).

### Immune module ratio

The IMR was defined as the ratio of the median expression of genes down-regulated in response to treatment [med($E_{down}$)] to the median expression of genes up-regulated in response to treatment [med($E_{up}$); Eq. 1]. The resulting measure is a unit-free measure of the host immune response over the treatment course.

$$\mathrm{IMR} = \frac{\mathrm{med}\left(E_{\mathrm{down}}\right)}{\mathrm{med}\left(E_{\mathrm{up}}\right)} \quad (1)$$

Three alternative groups of genes were used to calculate the IMR: (i) the full set of Sep3 genes, (ii) the treatment-responsive Sep3 genes that exhibited a significant regression coefficient with time, and (iii) a reduced set of 10 genes comprising the five most-strongly up-regulated and five most-strongly down-regulated at $T_R + 72$ hours.

### Gene clustering with correlation networks

A subset of 422 highly treatment-responsive genes, identified by at least one LMRM fixed effect coefficient adjusted *P* value $< 0.05$ and predicted $\log_2$(fold change) at $T_R + 72$ hours $>0.075$, underwent correlation network analysis to identify informative gene clusters. *P* value and $\log_2$(fold change) thresholds were chosen to ensure a sufficient number of genes were included in the analysis to identify underlying functional relationships. A gene coexpression network was derived using the WGCNA R package. Gene coexpression similarity was computed from raw intensity values for the selected genes at each of $T_R$, $T_R + 72$ hours, and $T_R + 5$ days, using the absolute Pearson correlation between gene expression profiles across patients. Coexpression similarity was transformed to a weighted topographical overlap matrix (*59*) using the function TOMsimilarityFromExpr. A soft threshold (power) β value of 10 was selected by evaluating a scale-free topology curve (fig. S15A) over threshold values from 1 to 20 and selecting a power resulting in a high scale-free fit index value (above 0.80). Average gene connectivity under alternative power values was also evaluated (fig. S15B). Gene networks were visualized using the igraph R package. An edge weight filter (topographical overlap values $\geq 0.12$) and a node topology filter ($\geq$5 neighbors within a distance of 2) were applied to eliminate peripherally connected nodes and aid visualization.

### Statistical analysis

Individual-level data are presented in data file S1. Comparisons of central tendency of a single measure between two groups were conducted using either a two-sided Student's *t* test, where the data met the test assumptions and were verified as normally distributed using a Shapiro-Wilk test, or a two-sided Wilcoxon signed-rank test; 95% CIs were calculated using a normal approximation. The independence of two categorical variables was evaluated using Fisher's exact test. Case versus control differential expression was determined

by linear modeling using the limma package (*60*). The Benjamini-Hochberg multiple testing correction was applied to calculate adjusted *P* values (*58*). Calculated *P* values for the significance of linear mixed regression coefficients were also adjusted using the Benjamini-Hochberg multiple testing correction. Correlation was measured using Pearson's correlation coefficient in cases where the data were continuous and met the test assumptions and using Spearman's rank correlation coefficient otherwise. Cell type quantification was conducted using the immunedeconv package (*61*) with the quanTIseq deconvolution algorithm (*35*) to compute cell fractions, and differences were tested for significance using a two-sided Wilcoxon signed-rank test. The significance threshold α was set at 0.05 for all statistical tests.

## Supplementary Materials

**The PDF file includes:**
Figs. S1 to S15
Tables S1 to S13
Legend for data file S1

**Other Supplementary Material for this manuscript includes the following:**
Data file S1
MDAR Reproducibility Checklist

## REFERENCES AND NOTES


1. M. Singer, C. S. Deutschman, C. W. Seymour, M. Shankar-Hari, D. Annane, M. Bauer, R. Bellomo, G. R. Bernard, J.-D. Chiche, C. M. Coopersmith, R. S. Hotchkiss, M. M. Levy, J. C. Marshall, G. S. Martin, S. M. Opal, G. D. Rubenfeld, T. van der Poll, J.-L. Vincent, D. C. Angus, The third international consensus definitions for sepsis and septic shock (Sepsis-3). *JAMA* **315**, 801–810 (2016).
2. T. Strunk, E. J. Molloy, A. Mishra, Z. A. Bhutta, Neonatal bacterial sepsis. *Lancet* **404**, 277–293 (2024).
3. B. J. Stoll, N. Hansen, A. A. Fanaroff, L. L. Wright, W. A. Carlo, R. A. Ehrenkranz, J. A. Lemons, E. F. Donovan, A. R. Stark, J. E. Tyson, W. Oh, C. R. Bauer, S. B. Korones, S. Shankaran, A. R. Laptook, D. K. Stevenson, L.-A. Papile, W. K. Poole, Late-onset sepsis in very low birth weight neonates: The experience of the NICHD neonatal research network. *Pediatrics* **110**, 285–291 (2002).
4. B. Cailes, C. Kortsalioudaki, J. Buttery, S. Pattnayak, A. Greenough, J. Matthes, A. B. Russell, N. Kennea, P. T. Heath, Epidemiology of UK neonatal infections: The neonIN infection surveillance network. *Arch. Dis. Child. Fetal Neonatal Ed.* **103**, F547–F553 (2018).
5. B. J. Stoll, N. I. Hansen, I. Adams-Chapman, A. A. Fanaroff, S. R. Hintz, B. Vohr, R. D. Higgins, Neurodevelopmental and growth impairment among extremely low-birth weight infants with neonatal infection. *JAMA* **292**, 2357–2365 (2004).
6. J. V. E. Brown, N. Meader, K. Wright, J. Cleminson, W. McGuire, Assessment of C-reactive protein diagnostic test accuracy for late-onset infection in newborn infants. *JAMA Pediatr.* **174**, 260–268 (2020).
7. G. Pontrelli, F. De Crescenzo, R. Buzzetti, A. Jenkner, S. Balduzzi, F. Calò Carducci, D. Amodio, M. De Luca, S. Chiurchiù, E. H. Davies, G. Copponi, A. Simonetti, E. Ferretti, V. Di Franco, V. Rasi, M. Della Corte, L. Gramatica, M. Ciabattini, S. Livadiotti, P. Rossi, Accuracy of serum procalcitonin for the diagnosis of sepsis in neonates and children with systemic inflammatory syndrome: A meta-analysis. *BMC Infect. Dis.* **17**, 302 (2017).
8. M. Chakraborty, P. R. Rodrigues, W. J. Watkins, A. Hayward, A. Sharma, R. Hayward, E. Smit, R. Jones, N. Goel, A. Asokkumar, J. Calvert, D. Odd, I. Morris, C. Doherty, S. Elliott, A. Strang, R. Andrews, S. Zaher, S. Sharma, S. Bell, S. Oruganti, C. Smith, J. Orme, S. Edkins, M. Craigon, D. White, W. Dantoft, L. C. Davies, L. Moet, J. E. McLaren, S. Clarkstone, G. L. Watson, K. Hood, S. Kotecha, B. P. Morgan, V. B. O'Donnell, P. Ghazal, NSeP: Immune and metabolic biomarkers for early detection of neonatal sepsis—Protocol for a prospective multicohort study. *BMJ Open* **11**, e050100 (2021).
9. H. A. H. Mahmoud, R. Parekh, S. Dhandibhotla, T. Sai, A. Pradhan, S. Alugula, M. Cevallos-Cueva, B. K. Hayes, S. Athanti, Z. Abdin, K. Basant, Insight into neonatal sepsis: An overview. *Cureus* **15**, e45530 (2023).
10. T. E. Sweeney, J. L. Wynn, M. Cernada, E. Serna, H. R. Wong, H. V. Baker, M. Vento, P. Khatri, Validation of the Sepsis MetaScore for diagnosis of neonatal sepsis. *J. Pediatr. Infect. Dis.* **7**, 129–135 (2018).
11. C. Chiesa, A. Panero, J. F. Osborn, A. F. Simonetti, L. Pacifico, Diagnosis of neonatal sepsis: A clinical and laboratory challenge. *Clin. Chem.* **50**, 279–287 (2004).
12. H. Wong, Sepsis biomarkers. *J. Pediatr. Intensive Care* **8**, 11–16 (2019).
13. C. L. Smith, P. Dickinson, T. Forster, M. Craigon, A. Ross, M. R. Khondoker, R. France, A. Ivens, D. J. Lynn, J. Orme, A. Jackson, P. Lacaze, K. L. Flanagan, B. J. Stenson, P. Ghazal, Identification of a human neonatal immune-metabolic network associated with bacterial infection. *Nat. Commun.* **5**, 4649 (2014).
14. L. McHugh, T. A. Seldon, R. A. Brandon, J. T. Kirk, A. Rapisarda, A. J. Sutherland, J. J. Presneill, D. J. Venter, J. Lipman, M. R. Thomas, P. M. C. K. Klouwenberg, L. van Vught, B. Scicluna, M. Bonten, O. L. Cremer, M. J. Schultz, T. van der Poll, T. D. Yager, R. B. Brandon, A molecular host response assay to discriminate between sepsis and infection negative systemic inflammation in critically ill patients: Discovery and validation in independent cohorts. *PLOS Med.* **12**, e1001916 (2015).
15. H. Wong, The pediatric sepsis biomarker risk model. *Crit. Care* **16**, R174 (2012).
16. T. E. Sweeney, A. Shidham, H. R. Wong, P. Khatri, A comprehensive time-course-based multicohort analysis of sepsis and sterile inflammation reveals a robust diagnostic gene set. *Sci. Transl. Med.* **7**, 287ra71 (2015).
17. E. Cano-Gamez, K. L. Burnham, C. Goh, A. Allcock, Z. H. Malick, L. Overend, A. Kwok, D. A. Smith, H. Peters-Sengers, D. Antcliffe, S. McKechnie, B. P. Scicluna, T. van der Poll, A. C. Gordon, C. J. Hinds, E. E. Davenport, J. C. Knight, N. Webster, H. Galley, J. Taylor, S. Hall, J. Addison, S. Roughton, H. Tennant, A. Guleri, N. Waddington, D. Arawwawala, J. Durcan, A. Short, K. Swan, S. Williams, S. Smolen, C. Mitchell-Inwang, T. Gordon, E. Errington, M. Templeton, P. Venatesh, G. Ward, M. McCauley, S. Baudouin, C. Higham, J. Soar, S. Grier, E. Hall, S. Brett, D. Kitson, R. Wilson, L. Mountford, J. Moreno, P. Hall, J. Hewlett, S. McKechnie, C. Garrard, J. Millo, D. Young, P. Hutton, P. Parsons, A. Smiths, R. Faras-Arraya, J. Soar, P. Raymode, J. Thompson, S. Bowrey, S. Kazembe, N. Rich, P. Andreou, D. Hales, E. Roberts, S. Fletcher, M. Rosbergen, G. Glister, J. M. Cuesta, J. Bion, J. Millar, E. J. Perry, H. Willis, N. Mitchell, S. Ruel, R. Carrera, J. Wilde, A. Nilson, S. Lees, A. Kapila, N. Jacques, J. Atkinson, A. Brown, H. Prowse, A. Krige, M. Bland, L. Bullock, D. Harrison, G. Mills, J. Humphreys, K. Armitage, S. Laha, J. Baldwin, A. Walsh, N. Doherty, S. Drage, L. O.-R. de Gordoa, S. Lowes, C. Higham, H. Walsh, V. Calder, C. Swan, H. Payne, D. Higgins, S. Andrews, S. Mappleback, C. Hind, C. Garrard, D. Watson, E. McLees, A. Purdy, M. Stotz, A. Ochelli-Okpue, S. Bonner, I. Whitehead, K. Hugil, V. Goodridge, L. Cawthor, M. Kuper, S. Pahary, G. Bellingan, R. Marshall, H. Montgomery, J. H. Ryu, G. Bercades, S. Boluda, A. Bentley, K. Mccalman, F. Jefferies, J. Knight, E. Davenport, K. Burnham, N. Maugeri, J. Radhakrishnan, Y. Mi, A. Allcock, C. Goh, An immune dysfunction score for stratification of patients with acute infection based on whole-blood gene expression. *Sci. Transl. Med.* **14**, eabq4433 (2022).
18. R. Yan, T. Zhou, Identification of key biomarkers in neonatal sepsis by integrated bioinformatics analysis and clinical validation. *Heliyon* **8**, e11634 (2022).
19. Y. Bai, N. Zhao, Z. Zhang, Y. Jia, G. Zhang, G. Dong, Identification and validation of a novel four-gene diagnostic model for neonatal early-onset sepsis with bacterial infection. *Eur. J. Pediatr.* **182**, 977–985 (2023).
20. N. P. Long, N. K. Phat, N. T. H. Yen, S. Park, Y. Park, Y. S. Cho, J. G. Shin, A 10-gene biosignature of tuberculosis treatment monitoring and treatment outcome prediction. *Tuberculosis* **131**, 102138 (2021).
21. A. Penn-Nicholson, S. K. Mbandi, E. Thompson, S. C. Mendelsohn, S. Suliman, N. N. Chegou, S. T. Malherbe, F. Darboe, M. Erasmus, W. A. Hanekom, N. Bilek, M. Fisher, S. H. Kaufmann, J. Winter, M. Murphy, R. Wood, C. Morrow, I. V. Rhijn, B. Moody, M. Murray, B. B. Andrade, T. R. Sterling, J. Sutherland, K. Naidoo, The Adolescent Cohort Study team, The GC6-74 Consortium, The SATVI Clinical and Laboratory Team, The ScreenTB Consortium, The AE-TBC Consortium, The RePORT Brazil Team, Peruvian Household Contacts Cohort Team, The CAPRISA IMPRESS team, RISK6, a 6-gene transcriptomic signature of TB disease risk, diagnosis and treatment response. *Sci. Rep.* **10**, 8629 (2020).
22. P. Schuetz, How to best use procalcitonin to diagnose infections and manage antibiotic treatment. *Clin. Chem. Lab. Med.* **61**, 822–828 (2023).
23. M. Stocker, M. Fontana, S. E. Helou, K. Wegscheider, T. M. Berger, Use of procalcitonin-guided decision-making to shorten antibiotic therapy in suspected neonatal early-onset sepsis: Prospective randomized intervention trial. *Neonatology* **97**, 165–174 (2010).
24. A. M. Rossum, R. W. Wulkan, A. M. Oudesluys-Murphy, Procalcitonin as an early marker of infection in neonates and children. *Lancet Infect. Dis.* **4**, 620–630 (2004).
25. X. Jiang, C. Zhang, Y. Pan, X. Cheng, W. Zhang, Effects of C-reactive protein trajectories of critically ill patients with sepsis on in-hospital mortality rate. *Sci. Rep.* **13**, 15223 (2023).
26. M.-Y. Lai, M.-H. Tsai, C.-W. Lee, M.-C. Chiang, R. Lien, R.-H. Fu, H.-R. Huang, S.-M. Chu, J.-F. Hsu, Characteristics of neonates with culture-proven bloodstream infection who have low levels of C-reactive protein (≤10 mg/l). *BMC Infect. Dis.* **15**, 320 (2015).
27. M. B. Dhudasia, W. E. Benitz, D. D. Flannery, L. Christ, D. Rub, G. Remaschi, K. M. Puopolo, S. Mukhopadhyay, Diagnostic performance and patient outcomes with C-reactive protein use in early-onset sepsis evaluations. *J. Pediatr.* **256**, 98–104.e6 (2023).

28. L. F. Hill, M. N. Clements, M. A. Turner, D. Donà, I. Lutsar, E. Jacqz-Aigrain, P. T. Heath, E. Roilides, L. Rawcliffe, C. Alonso-Diaz, E. Baraldi, A. Dotta, M. L. Ilmoja, A. Mahaveer, T. Metsvaht, G. Mitsiakos, V. Papaevangelou, K. Sarafidis, A. S. Walker, M. Sharland, M. Clements, B. Bafadal, A. A. Allen, F. Anatolitou, A. D. Vecchio, M. Giuffrè, K. Karachristou, P. Manzoni, S. Martinelli, P. Moriarty, A. Nika, V. Papaevangelou, C. Roehr, L. S. Alcobendas, T. Siahanidou, C. Tzialla, L. Bonadies, N. Booth, P. C. Morales-Betancourt, M. Cordeiro, C. de Alba Romero, J. de la Cruz, M. D. Luca, D. Farina, C. Franco, D. Gialamprinou, M. Hallik, L. Ilardi, V. Insinga, E. Iosifidis, R. Kalamees, A. Kontou, Z. Molnar, E. Nikaina, C. Petropoulou, M. Reyne, K. Tataropoulou, P. Triantafyllidou, A. Vontzalidis, M. Sharland, Optimised versus standard dosing of vancomycin in infants with Gram-positive sepsis (NeoVanc): A multicentre, randomised, open-label, phase 2b, non-inferiority trial. *Lancet Child Adolesc. Health* **6**, 49–59 (2022).
29. C. Stockmann, M. G. Spigarelli, S. C. Campbell, J. E. Constance, J. D. Courter, E. A. Thorell, J. Olson, C. M. T. Sherwin, Considerations in the pharmacologic treatment and prevention of neonatal sepsis. *Pediatr. Drugs* **16**, 67–81 (2014).
30. M. Lauss, A. Frigyesi, T. Ryden, M. Höglund, Robust assignment of cancer subtypes from expression data using a univariate gene expression average as classifier. *BMC Cancer* **10**, 532 (2010).
31. A. K. Turnbull, R. R. Kitchen, A. A. Larionov, L. Renshaw, J. M. Dixon, A. H. Sims, Direct integration of intensity-level data from Affymetrix and Illumina microarrays improves statistical power for robust reanalysis. *BMC Med. Genomics* **5**, 35 (2012).
32. H. R. Wong, N. Cvijanovich, G. L. Allen, R. Lin, N. Anas, K. Meyer, R. J. Freishtat, M. Monaco, K. Odoms, B. Sakthivel, T. P. Shanley, Genomic expression profiling across the pediatric systemic inflammatory response syndrome, sepsis, and septic shock spectrum. *Crit. Care Med.* **37**, 1558–1566 (2009).
33. F. Venet, J. Schilling, M. A. Cazalis, J. Demaret, F. Poujol, T. Girardot, C. Rouget, A. Pachot, A. Lepape, A. Friggeri, T. Rimmelé, G. Monneret, J. Textoris, Modulation of LILRB2 protein and mRNA expressions in septic shock patients and after ex vivo lipopolysaccharide stimulation. *Hum. Immunol.* **78**, 441–450 (2017).
34. F. Abdallah, S. Coindre, M. Gardet, F. Meurisse, A. Naji, N. Suganuma, L. Abi-Rached, O. Lambotte, B. Favier, Leukocyte immunoglobulin-like receptors in regulating the immune response in infectious diseases: A window of opportunity to pathogen persistence and a sound target in therapeutics. *Front. Immunol.* **12**, 717998 (2021).
35. F. Finotello, C. Mayer, C. Plattner, G. Laschober, D. Rieder, H. Hackl, A. Krogsdam, Z. Loncova, W. Posch, D. Wilflingseder, S. Sopper, M. Ijsselsteijn, T. P. Brouwer, D. Johnson, Y. Xu, Y. Wang, M. E. Sanders, M. V. Estrada, P. Ericsson-Gonzalez, P. Charoentong, J. Balko, N. F. D. C. C. D. Miranda, Z. Trajanoski, Molecular and pharmacological modulators of the tumor immune contexture revealed by deconvolution of RNA-seq data. *Genome Med.* **11**, 34 (2019).
36. D. Harbeson, F. Francis, W. Bao, N. A. Amenyogbe, T. R. Kollmann, Energy demands of early life drive a disease tolerant phenotype and dictate outcome in neonatal bacterial sepsis. *Front. Immunol.* **9**, 1918 (2018).
37. J. E. Hibbert, A. Currie, T. Strunk, Sepsis-induced immunosuppression in neonates. *Front. Pediatr.* **6**, 357 (2018).
38. D. I. Kotov, O. V. Lee, S. A. Fattinger, C. A. Langner, J. V. Guillen, J. M. Peters, A. Moon, E. M. Burd, K. C. Witt, D. B. Stetson, D. L. Jaye, B. D. Bryson, R. E. Vance, Early cellular mechanisms of type I interferon-driven susceptibility to tuberculosis. *Cell* **186**, 5536–5553.e22 (2023).
39. G. Trinchieri, Type I interferon: Friend or foe? *J. Exp. Med.* **207**, 2053–2063 (2010).
40. R. M. B. Teles, T. G. Graeber, S. R. Krutzik, D. Montoya, M. Schenk, D. J. Lee, E. Komisopoulou, K. Kelly-Scumpia, R. Chun, S. S. Iyer, E. N. Sarno, T. H. Rea, M. Hewison, J. S. Adams, S. J. Popper, D. A. Relman, S. Stenger, B. R. Bloom, G. Cheng, R. L. Modlin, Type I interferon suppresses type II interferon–triggered human anti-mycobacterial responses. *Science* **339**, 1448–1453 (2013).
41. S. Ming, M. Li, M. Wu, J. Zhang, H. Zhong, J. Chen, Y. Huang, J. Bai, L. Huang, J. Chen, Q. Lin, J. Liu, J. Tao, D. He, X. Huang, Immunoglobulin-like transcript 5 inhibits macrophage-mediated bacterial killing and antigen presentation during sepsis. *J. Infect. Dis.* **220**, 1688–1699 (2019).
42. M. Nakayama, K. Kurokawa, K. Nakamura, B. L. Lee, K. Sekimizu, H. Kubagawa, K. Hiramatsu, H. Yagita, K. Okumura, T. Takai, D. M. Underhill, A. Aderem, K. Ogasawara, Inhibitory receptor paired Ig-like receptor B is exploited by *Staphylococcus aureus* for virulence. *J. Immunol.* **189**, 5903–5911 (2012).
43. Y. Zhao, E. van Woudenbergh, J. Zhu, A. J. R. Heck, K. P. M. van Kessel, C. J. C. de Haas, P. C. Aerts, J. A. G. van Strijp, A. J. McCarthy, The orphan immune receptor LILRB3 modulates Fc receptor–mediated functions of neutrophils. *J. Immunol.* **204**, 954–966 (2020).
44. H. T. T. Gander-Bui, J. Schlafli, J. Baumgartner, S. Walthert, V. Genitsch, G. van Geest, J. A. Galván, C. Cardozo, C. G. Martinez, M. Grans, S. Muth, R. Bruggmann, H. C. Probst, C. Gabay, S. Freigang, Targeted removal of macrophage-secreted interleukin-1 receptor antagonist protects against lethal candida albicans sepsis. *Immunity* **56**, 1743–1760.e9 (2023).
45. L. F. Hill, M. A. Turner, I. Lutsar, P. T. Heath, P. Hardy, L. Linsell, E. Jacqz-Aigrain, E. Roilides, M. Sharland, C. Giaquinto, D. Bilardi, T. Planche, T. M. Huertas, W. Hope, W. Zhao, P. Ghazal, A. Dotta, J. D. L. Cruz, C. A. Diáz, S. Conroy, L. Rawcliffe, D. Bonifazi, C. Manfredi, M. Felisi, An optimised dosing regimen versus a standard dosing regimen of vancomycin for the treatment of late onset sepsis due to Gram-positive microorganisms in neonates and infants aged less than 90 days (NeoVanc): Study protocol for a randomised controlled trial. *Trials* **21**, 329 (2020).
46. A. Kauffmann, R. Gentleman, W. Huber, arrayQualityMetrics—A Bioconductor package for quality assessment of microarray data. *Bioinformatics* **25**, 415–416 (2009).
47. J. W. Tukey, *Exploratory Data Analysis*, Addison-Wesley Series in Behavioral Sciences: Quantitative Methods (Addison-Wesley, 1977).
48. B. S. Carvalho, R. A. Irizarry, A framework for oligonucleotide microarray preprocessing. *Bioinformatics* **26**, 2363–2367 (2010).
49. J. W. MacDonald, affycoretools: Functions useful for those doing repetitive analyses with Affymetrix genechips (2022).
50. J. W. MacDonald, clariomdhumantranscriptcluster.db: Affymetrix clariomdhuman annotation data (chip clariomdhumantranscriptcluster). R package version 8.8.0 (2021).
51. A. Kauffmann, W. Huber, Microarray data quality control improves the detection of differentially expressed genes. *Genomics* **95**, 138–142 (2010).
52. B. Klaus, S. Reisenauer, An end to end workflow for differential gene expression using Affymetrix microarrays. *F1000Res.* **5**, 1384 (2018).
53. Ensembl Project, Ensembl (2021); http://ensembl.org/info/data/ftp/index.html/.
54. M. Carlson, hgu133plus2.db: Affymetrix human genome u133 plus 2.0 array annotation data (chip hgu133plus2). R package version 3.2.3 (2016).
55. D. Bates, M. Mächler, B. M. Bolker, S. C. Walker, Fitting linear mixed-effects models using lme4. *J. Stat. Softw.* **67**, 1–48 (2015).
56. A. Kuznetsova, P. B. Brockhoff, R. H. B. Christensen, lmerTest package: Tests in linear mixed effects models. *J. Stat. Softw.* **82**, 1–26 (2017).
57. D. J. Barr, R. Levy, C. Scheepers, H. J. Tily, Random effects structure for confirmatory hypothesis testing: Keep it maximal. *J. Mem. Lang.* **68**, 255–278 (2013).
58. Y. Benjamini, Y. Hochberg, Controlling the false discovery rate: A practical and powerful approach to multiple testing. *J. R. Stat. Soc. B. Methodol.* **57**, 289–300 (1995).
59. B. Zhang, S. Horvath, A general framework for weighted gene co-expression network analysis. *Stat. Appl. Genet. Mol. Biol.* **4**, 17 (2005).
60. M. E. Ritchie, B. Phipson, D. Wu, Y. Hu, C. W. Law, W. Shi, G. K. Smyth, Limma powers differential expression analyses for RNA-sequencing and microarray studies. *Nucleic Acids Res.* **43**, e47 (2015).
61. G. Sturm, F. Finotello, F. Petitprez, J. D. Zhang, J. Baumbach, W. H. Fridman, M. List, T. Aneichyk, Comprehensive evaluation of transcriptome-based cell-type quantification methods for immuno-oncology. *Bioinformatics* **35**, i436–i445 (2019).


**Acknowledgments:** This article is dedicated to Peter Ghazal, our expert colleague and collaborator, mentor, inspiration, and very dear late friend. We thank the parents and guardians of patients and investigators from the centers who participated in the NeoVanc study. We thank the sponsor, Fondazione Penta, and the independent data monitoring committee (J. van den Anker, J. Gray, and C. Chazallon). We also thank the late Hector Wong for providing detailed metadata for the pediatric validation cohort (GSE13904). **Funding:** This work was supported by the European Union Seventh Framework Programme for research, technological development, and demonstration under grant agreement no. 602041 (to L.F.H., M.N.C., P.T.H., and M.S.) and a Ser Cymru grant from the Welsh government and EU/ERDF funds (to P.G.). **Author contributions:** This study was conceptualized and designed by P.G. and E.C.P. Funding was acquired by P.G., I.L., M.A.T., E.R., P.T.H., and M.S. The data collection methodology was developed by P.G., L.F.H., and P.T.H. The NeoVanc principal and coinvestigators performed the participant recruitment and data collection. Participant recruitment and data collection were supervised by I.L., M.A.T., and E.R. L.F.H. and M.N.C. maintained and curated NeoVanc trial data. Microbiology analysis was overseen by L.F.H. Study materials and resources were coordinated by L.F.H., S.E., and R.A. S.E. managed microarray sample preparation, quality assurance, and data generation. E.C.P. curated the validation datasets. P.G., E.C.P., and W.J.W. developed the analytical methodology. E.C.P. performed all data preprocessing, formal data analysis, custom code development, and visualization. R.A. provided bioinformatics resources. Data interpretation was performed by E.C.P., P.G., L.F.H., W.J.W., and J.E.M. Data validation was undertaken by E.C.P. and W.J.W. The project was supervised and overseen by P.G., M.S., P.T.H., and L.F.H. at all stages. E.C.P, F.L., W.J.W., and J.E.M. supervised data analysis and manuscript writing. Writing of the original manuscript was performed by E.C.P. Reviewing and editing the manuscript was performed by all authors. **Competing interests:** P.T.H. is a member of the National Institute for Health and Care Excellence neonatal infection guideline development group. P.G. is an inventor on a patent (US Patent No. 10851415 B2, Molecular Predictors of Sepsis) related to the Sep3 biomarkers described in this manuscript. All other authors declare that they have no competing interests. **Data and materials availability:** All data associated with this study are provided in the paper or the Supplementary Materials. Gene expression data for NeoVanc samples used in this study are publicly available in ArrayExpress (accession number: E-MTAB-15687). Accession numbers for all public datasets used are provided in Materials and Methods. Custom code and supplementary metadata required to generate the results in this study are deposited at Zenodo, available at 10.5281/zenodo.17251047. Sharing of data related to the NeoVanc trial beyond that used in this study will be considered on the basis of a detailed proposal, which should include aims, methods, and a statistical analysis plan. Requests will be checked for compatibility with regulatory and

ethics committee requirements and with participant informed consent. Proposals should be addressed to L.F.H. at lhill@sgul.ac.uk and will be evaluated by the sponsor.

**NeoVanc Consortium** In addition to the NeoVanc Consortium members who are listed as authors (E.C.P., W.J.W., S.E., J.E.M, M.N.C., R.A., F.L., I.L., M.A.T., E.R., P.T.H., M.S., L.F.H., and P.G.), the following are NeoVanc Consortium members who acted as country coordinators, principal investigators, or coinvestigators who have contributed to participant recruitment and data collection and to trial oversight and coordination:

Tatiana Munera Huertas[7], Uzma Khan[7], Mari-Liis Ilmoja[8], Maarja Hallik[8], Tuuli Metsvaht[9], Riste Kalamees[9], Korina Karachristou[10], Adamantios Vontzalidis[10], Fani Anatolitou[10], Chryssoula Petropoulou[10], Tania Siahanidou[10], Eirini Nikaina[10], Vassiliki Papaevangelou[11], Pinelopi Triantafyllidou[11], Kosmas Sarafidis[12], Angeliki Kontou[12], Angeliki Nika[13], Kassandra Tataropoulou[13], George Mitsiakos[14], Elias Iosifidis[14], Dimitra Gialamprinou[14], Stefano Martinelli[15], Laura Ilardi[15], Eugenio Baraldi[16], Luca Bonadies[16], Antonio Del Vecchio[17], Caterina Franco[17], Andrea Dotta[18], Maia De Luca[18], Chryssoula Tzialla[19], Clara Alonso-Diaz[20], Concepción de Alba Romero[20], Javier de la Cruz[20], Paola Catalina Morales-Betancourt[20], Ana Alarcon Allen[21], Mar Reyné[21], Ajit Mahaveer[22], Nicola Booth[22], Davide Bilardi[23], Daniele Donà[23], Louise Rawcliffe[24], Basma Bafadal[24], Deborah Roberts[24], Antonella Silvestri[24], Cristina Manfredi[25], Mariagrazia Felisi[25], Paola Gandini[25]

Affiliations 1 to 7 can be found at the beginning of the paper.

[8]Tallinn Children's Hospital, 13419 Tallinn, Estonia. [9]Tartu University Hospital, 50406 Tartu, Estonia. [10]Aghia Sophia Children's Hospital, 115 27 Athens, Greece. [11]General University Hospital, Attikon, 124 62 Chaïdári, Greece. [12]Hippokration Hospital, 546 42 Thessaloniki, Greece. [13]Kyriakou Children's Hospital, 115 27 Athens, Greece. [14]Papageorgiou Hospital, 564 29 Thessaloniki, Greece. [15]ASST Grande Ospedale Metropolitano Niguarda, 20162 Milan, Italy. [16]Azienda Ospedale-Universita' di Padova, Fondazione Istituto di Ricerca Pediatrica, 35128 Padova, Italy. [17]Ospedale Di Venere, 70131 Bari, Italy. [18]Ospedale Pediatrico Bambino Gesù, 00165 Rome, Italy. [19]Policlinico San Matteo, 27100 Pavia, Italy. [20]Hospital Universitario 12 de Octubre, 28041 Madrid, Spain. [21]Hospital Sant Joan de Deu, 08950 Barcelona, Spain. [22]St Mary's Hospital, Manchester M13 0JH, UK. [23]Fondazione Penta–ONLUS, 35127 Padova, Italy. [24]Therakind Ltd., London N3 2JX, UK. [25]Consorzio per Valutazioni Biologiche e Farmacologiche, 27100 Pavia, Italy.

Submitted 18 October 2024
Resubmitted 21 May 2025
Accepted 17 October 2025
Published 26 November 2025
10.1126/scitranslmed.adt1938